ANL-ART-114

FY 2017 Status of Sodium Freezing and Remelting Tests

Nuclear Engineering Division

About Argonne National Laboratory
Argonne is a U.S. Department of Energy laboratory managed by UChicago Argonne, LLC under contract DE-AC02-06CH11357. The Laboratory's main facility is outside Chicago, at 9700 South Cass Avenue, Argonne, Illinois 60439. For information about Argonne and its pioneering science and technology programs, see www.anl.gov.

DOCUMENT AVAILABILITY

Online Access: U.S. Department of Energy (DOE) reports produced after 1991 and a growing number of pre-1991 documents are available free via DOE's SciTech Connect (http://www.osti.gov/scitech/)

Reports not in digital format may be purchased by the public from the National Technical Information Service (NTIS):

U.S. Department of Commerce
National Technical Information Service
5301 Shawnee Rd
Alexandra, VA 22312
www.ntis.gov
Phone: (800) 553-NTIS (6847) or (703) 605-6000
Fax: (703) 605-6900
Email: **orders@ntis.gov**

Reports not in digital format are available to DOE and DOE contractors from the Office of Scientific and Technical Information (OSTI):

U.S. Department of Energy
Office of Scientific and Technical Information
P.O. Box 62
Oak Ridge, TN 37831-0062
www.osti.gov
Phone: (865) 576-8401
Fax: (865) 576-5728

Disclaimer
This report was prepared as an account of work sponsored by an agency of the United States Government. Neither the United States Government nor any agency thereof, nor UChicago Argonne, LLC, nor any of their employees or officers, makes any warranty, express or implied, or assumes any legal liability or responsibility for the accuracy, completeness, or usefulness of any information, apparatus, product, or process disclosed, or represents that its use would not infringe privately owned rights. Reference herein to any specific commercial product, process, or service by trade name, trademark, manufacturer, or otherwise, does not necessarily constitute or imply its endorsement, recommendation, or favoring by the United States Government or any agency thereof. The views and opinions of document authors expressed herein do not necessarily state or reflect those of the United States Government or any agency thereof, Argonne National Laboratory, or UChicago Argonne, LLC

ANL-ART-114

FY 2017 Status of Sodium Freezing and Remelting Tests

prepared by
Q. Lv, E. Boron, Y. Momozaki, D. B. Chojnowski, J. J. Sienicki, and C. B. Reed
Nuclear Engineering Division, Argonne National Laboratory

September 15, 2017

ABSTRACT

The Sodium Freezing and Remelting experiment facility at Argonne National Laboratory has been significantly modified and improved. The main improvement was replacement of the two original stainless steel test sections that had strain gages limited by their bonds to the stainless steel to maximum temperatures of 350°C with a single new test section with strain gages that can be utilized up to 980°C and a thin wall to enhance measured strains. Wetting of stainless steel by sodium within a practical time of one to a few days is expected to require temperatures of 450°C or greater. Thus, the higher temperature strain gages enable wetting in a short time of a few days. Wetting below 350°C would have required an impractically long time of at least weeks. Other improvements included upgrading of the loop configuration, incorporation of a cold finger to purify sodium, a new data acquisition system, and reinstallation of the many heaters, heater controllers, and thermocouples. After the loop had been heated to 400°C for about two hours, an initial sodium freezing test was conducted. It is thought that the sodium might have at least partially wetted the stainless steel wall under these conditions. The strain gage measurements indicate that an incremental step inward deformation of the test section thin wall occurred as the temperature decreased through the sodium freezing temperature. This behavior is consistent with sodium initially adhering to the stainless steel inner wall but breaking away from the wall as the freezing sodium contracted. Conduct of additional sodium freezing tests under well wetted conditions was prevented as a result of stoppage of all electrical work at Argonne by the Laboratory Director on July 25, 2017. A pathway to resuming electrical work is now in place at Argonne and additional sodium freezing testing will resume next fiscal year.

Table of Contents

Abstract i
List of Figures iv
List of Tables vi
1 Introduction 7
2 Objectives 9
3 Sodium Freezing and Remelting Test Facility Description 10
3.1 Modifications/Upgrades to the Sodium Freezing and Remelting Test Facility 11
3.1.1 Test Section 12
3.1.2 Electromagnetic (EM) Pump and Power Supply 22
3.1.3 Heating System 24
3.1.4 Thermocouple Instrumentation 26
3.1.5 Data Acquisition System 27
3.1.6 Electrical Connection 27
3.2 Sodium Reservoir 28
3.3 Cold Finger 29
4 Baseline Tests 35
4.1 Strain Gage Balance Test 35
4.2 Strain Gage Pressure Response Test 35
4.3 Strain Gage Temperature Response Test 36
5 Shakedown Test 39
6 First Freezing Test at ~ 400°C 40
7 Summary 47
Acknowledgements 48
References 49

LIST OF FIGURES

Figure 1. Upgraded Sodium Freezing and Remelting test facility 10
Figure 2. CAD drawing of the upgraded Sodium Freezing and Remelting test facility, not including the cold finger 11
Figure 3. The Sodium Freezing and Remelting test facility before modifications/upgrades 12
Figure 4. Fabrication drawing of the new test section 13
Figure 5. Initial design of connecting the test section to the loop using tube coils 16
Figure 6. Temperature distribution for thermal study Case 1 17
Figure 7. Temperature distribution for thermal study Case 2 18
Figure 8. Stress results for Case 1 19
Figure 9. Strain results for Case 1 19
Figure 10. Stress results for Case 2 20
Figure 11. Strain results for Case 2 20
Figure 12. Stress results for Case 3 21
Figure 13. Strain results for Case 3 21
Figure 14. Stress results for Case 4 22
Figure 15. Strain results for Case 4 22
Figure 16. Drawing of EM pump duct and copper electrodes (left), and EM pump duct and electrode assembly after nickel plating 23
Figure 17. Picture showing the orientation of the EM pump 24
Figure 18. Ceramic band heaters 25
Figure 19. Front panel of heater control system for Zones 1-6 (picture taken during the ~ 400ºC test performed in FY 2017) 25
Figure 20. Updated heating zones for the Freezing and Remelting test facility 26
Figure 21. Layout of the instrumented thermocouples 27
Figure 22. Installed electrical enclosure for better electrical shielding 28
Figure 23. Section View (Left), Sectioned Duplicates of Components Comprising the Sodium Fill Reservoir (Center) and Fabricated Reservoir (Right) 29
Figure 24. Cold finger fabrication drawing 30
Figure 25. Cold finger top flange 31
Figure 26. Cold finger bellows drawing 32
Figure 27. Cold finger assembly 33
Figure 28. Cold finger top view 33
Figure 29. Cold finger air inlet/outlet 34
Figure 30. Strain gage pressure response test results 36
Figure 31. Setup of the strain gage temperature response test 37
Figure 32. Temperature response test results for the two strain gages at + 4.8” 37
Figure 33. Temperature response test results for the two strain gages at the center 38
Figure 34. Temperature response test results for the two strain gages at - 4.8” 38
Figure 35. System temperatures before and after turning on the EM pump 39
Figure 36. Test section maintained at ~ 400°C for ~ 2 hours 41
Figure 37. Propagation of freezing front from the ends toward the center of the test section 42
Figure 38. Axial strain vs temperature at –4.8” from the test section center 42
Figure 39. Hoop strain vs temperature at -4.8” from the test section center 43
Figure 40. Axial strain vs temperature at +4.8” from the test section center 43

Figure 41. Hoop strain vs temperature at +4.8” from the test section center..... 44
Figure 42. Axial Strain 1 vs temperature at the test section center..... 44
Figure 43. Axial Strain 2 vs temperature at the test section center..... 45
Figure 44. Hoop Strain 1 vs temperature at the test section center..... 45
Figure 45. Hoop Strain 2 vs temperature at the test section center..... 46

LIST OF TABLES

Table 1. Detailed layout of the thermocouples on the test section..... 14
Table 2. Detailed layout of the strain gages on the test section..... 15
Table 3. Strain gage balance test results..... 35

1 Introduction

Research and development on advanced energy conversion systems for Sodium-Cooled Fast Reactors (SFRs) is being carried out to identify energy conversion approaches that offer capital cost, safety, and efficiency benefits beyond the current Rankine superheated steam cycle. The current focus in the U.S. is on the supercritical carbon dioxide (sCO_2) Brayton cycle. The sCO_2 Brayton cycle is well suited for application to SFRs. The cycle is highly recuperated and will operate with a CO_2 temperature rise through the sodium-to-CO_2 heat exchanger of about 150°C. This is approximately equal to the temperature rise through the SFR core, providing an excellent match.

The sCO_2 Brayton cycle offers a number of benefits over the traditional Rankine superheated steam cycle. Foremost is eliminating sodium-water reactions. Sodium reacts energetically with water releasing heat and generating combustible hydrogen gas. With the Rankine water/steam cycle, the designer must incorporate design features for sodium-heated steam generators to detect small leakages of water/steam into sodium before the leaks grow in size and to accommodate sodium-water reactions following the postulated double-ended guillotine rupture of a steam generator tube failure. Those design features add to the capital cost of the SFR. While the sCO_2 Brayton cycle eliminates sodium-water reactions, there is a need to understand and accommodate the effects of sodium-CO_2 interactions.

The sCO_2 Brayton cycle offers the potential for lower capital cost than the Rankine steam cycle. The sCO_2 cycle provides higher cycle efficiency than the steam cycle for higher SFR core outlet temperatures further reducing the plant cost per unit electrical power and increasing the plant net present value. The sCO_2 cycle turbomachinery is remarkably small giving rise to the expectation of significant cost savings provided that reliable and cost effective compact heat exchangers can be utilized for the sodium-to-CO_2 heat exchangers, high temperature recuperator, low temperature recuperator, and CO_2-to-water cooler.

Utilization of the sCO_2 Brayton cycle requires that suitably reliable and economical sodium-to-CO_2 heat exchangers are designed. Development of the sCO_2 cycle at Argonne National Laboratory (Argonne) envisions use of compact diffusion-bonded heat exchangers such as those manufactured by Heatric Division of Meggitt (UK) Ltd [1,2]. Heat transfer from sodium to sCO_2 does not involve boiling as with the steam cycle such that heat transfer can take place inside of compact diffusion-bonded heat exchangers. Compact diffusion-bonded heat exchangers potentially offer high reliability in terms of the expectation of a low failure rate. Compact diffusion-bonded heat exchangers also offer long life and significantly smaller volume relative to other heat exchanger types.

In the Argonne AFR-100 SFR design developed under the Advanced Reactor Technologies Program, sodium enters the sodium-to-CO_2 heat exchangers at 528°C and exits at 373°C. At these temperatures, the heat exchanger stainless steel is expected to be wetted by the sodium within days. In reality, the heat exchanger would likely already have been wetted from exposure to sodium at lower temperatures of about 200°C during the lengthy startup of the reactor.

The utilization of compact diffusion-bonded sodium-to-CO_2 heat exchangers requires that fundamental phenomena for such heat exchangers be understood. This will enable heat exchangers to be reliably designed for the complete spectrum of normal and off-normal transient operating conditions. Three particular phenomena that have been identified for which knowledge and understanding are crucial are:

- Thermal shock-induced failure of the heat exchanger;
- Failure to efficiently drain sodium from heat exchanger sodium channels; and
- Heat exchanger failure due to freezing or melting of inadvertently trapped sodium remaining inside of heat exchanger sodium channels following draining.

To investigate and gain knowledge and understanding of the third phenomenon listed above, a Sodium Freezing and Remelting test facility has been designed and built at Argonne. The sodium freezing and remelting campaign dates back to FY 2010 [3] when the concept for an experimental test facility was developed. In FY 2011 [4], it was decided to design and assemble a small-scale facility for fundamental sodium freezing and remelting testing. In parallel, the formulation and design of fundamental sodium freezing experiments to conduct in the sodium freezing and remelting facility was undertaken. To this end, an investigation into the fundamental freezing and remelting behavior of sodium inside of stainless steel channels was undertaken using analytical models. In FY 2012 [5], the Sodium Freezing and Remelting test facility was designed, fabricated, and assembled; and shakedown tests were initiated. From FY 2013 to FY 2016 [6,7], the shakedown tests were continued and a series of freezing and remelting tests were performed. Due to the temperature limits of the strain gages implemented on the test sections, those experiments were limited to 300ºC and did not reach wetting of the test section inner surface, a critical phenomenon that needs to be achieved in order to observe excess stress/strain when sodium freezing/melting occurs. This limitation was due to specification of the wrong bonding material to attach the strain gages to the stainless steel test sections. The bonding material was limited to 350ºC.

It was therefore decided to replace the old test sections with a new design with high-temperature strain gages (temperature limit of 980ºC) implemented. The design of the new single test section incorporates a thin wall to enhance the strains achieved. In FY 2017, the work was focused on replacing the old test sections with the new test section. Due to the existing sodium inside the test loop, the replacement work had to be performed carefully to avoid contaminating the sodium. A series of baseline tests on the new test section, including pressure response tests, temperature response tests, and strain gage balance tests were performed before and after the new test section installation. These tests provide useful baseline data for correction and troubleshooting that may be needed for subsequent formal tests. Upon completion of the new test section installation, a shakedown test at ~ 200ºC was performed, mainly to confirm the availability of sodium flow. Following that, a formal test at ~ 400ºC in the test section was performed. In this report, details of the work performed in FY 2017 will be discussed.

2 Objectives

The overall objective of the sodium freezing and remelting tests is to characterize the stress that can develop in stainless steel components containing freezing sodium through adhesion between the component and the sodium. The stresses result due to differential thermal expansion and in particular due to the fact that sodium has a significantly larger thermal expansion coefficient than stainless steel. Below sodium's melting point, the CTE of 316 SS is only ~16 μm/m•K while for sodium it is ~ 75 μm/m•K. Therefore, during freezing, as well as during subsequent cooling after freezing, the solid sodium will contract at a faster rate than stainless steel such that tensile stresses could develop within the sodium and at the sodium-stainless steel interface, if the sodium is well wetted to the metal surface. The tests using the apparatus described here are intended to allow the measurement of the maximum tensile stresses that can be developed in the sodium and the maximum interfacial stresses that can be developed between the sodium and the stainless steel component. To understand the stresses that could develop, a better understanding of the freezing behavior of sodium and the interaction with stainless steel components is necessary.

From FY 2013 to FY 2016 [6,7], a series of freezing and remelting tests were performed. Due to the temperature limits of the strain gages implemented on the test sections, however, those experiments were not able to reach wetting of the test section inner surface. Therefore, the expected phenomenon of abrupt change in the strain during sodium freezing was not observed in previous tests. It was therefore decided to replace the old test sections with a new thin wall design with high-temperature strain gages (temperature limit of 980ºC) implemented. The use of the high-temperature strain gages will enable the test facility to be operated at higher temperatures above 400ºC to facilitate the wetting of the test section inner surface.

There are two main objectives for FY 2017:

- Complete the replacement of the old test sections with the new thin-walled test section with high temperature strain gages and thermocouples, and bring the test facility back into operation; and
- Initiate the sodium freezing and remelting tests.

3 Sodium Freezing and Remelting Test Facility Description

The upgraded Freezing and Remelting test facility, as shown in Figure 1 and Figure 2, is a simple closed loop system only partially filled with sodium. This test facility consists of four main components: the test section in the bottom, the DC EM pump located in the small vertical leg, the sodium reservoir located in the opposite leg, and the cold finger submerged into the sodium reservoir. The small tubing, including the pump duct, is ½ inch outer diameter (OD) tubing; the fill reservoir is made from a 4-inch Schedule 80 pipe. Swagelok VCR fittings are used on all non-welded connections, except the top flange for the sodium reservoir. The system must be vacuum tight for bake-out prior to the initial sodium loading, so the top flange is sealed with a Conflat knife-edge seal design. The sodium freezing and remelting test section is connected using quick change VCR fittings to elbows below the sodium fill reservoir and the electromagnetic sodium pump. The cold finger is submerged in the sodium reservoir, and sealed to the reservoir cap with a conflat flange.

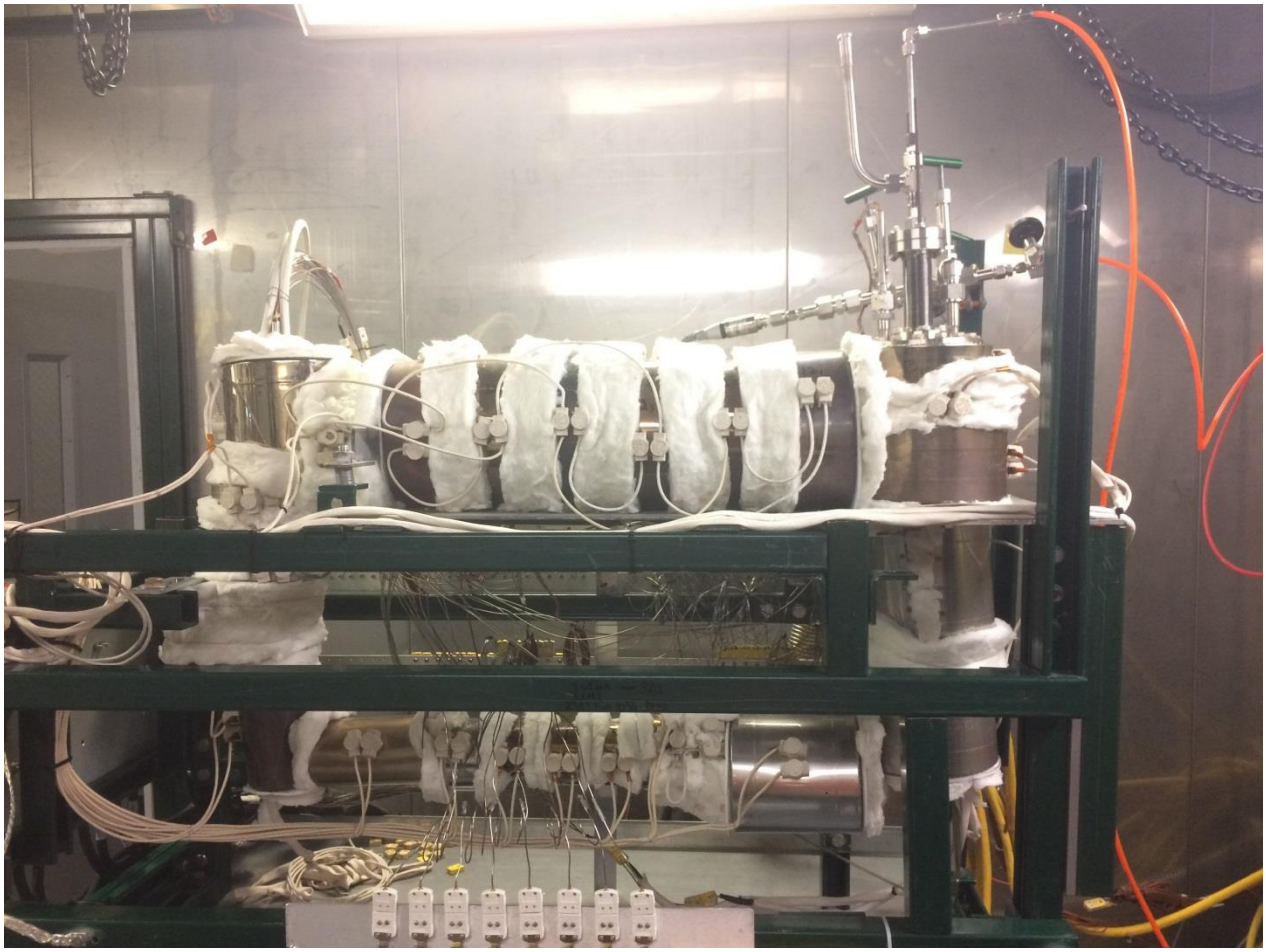

Figure 1. Upgraded Sodium Freezing and Remelting test facility

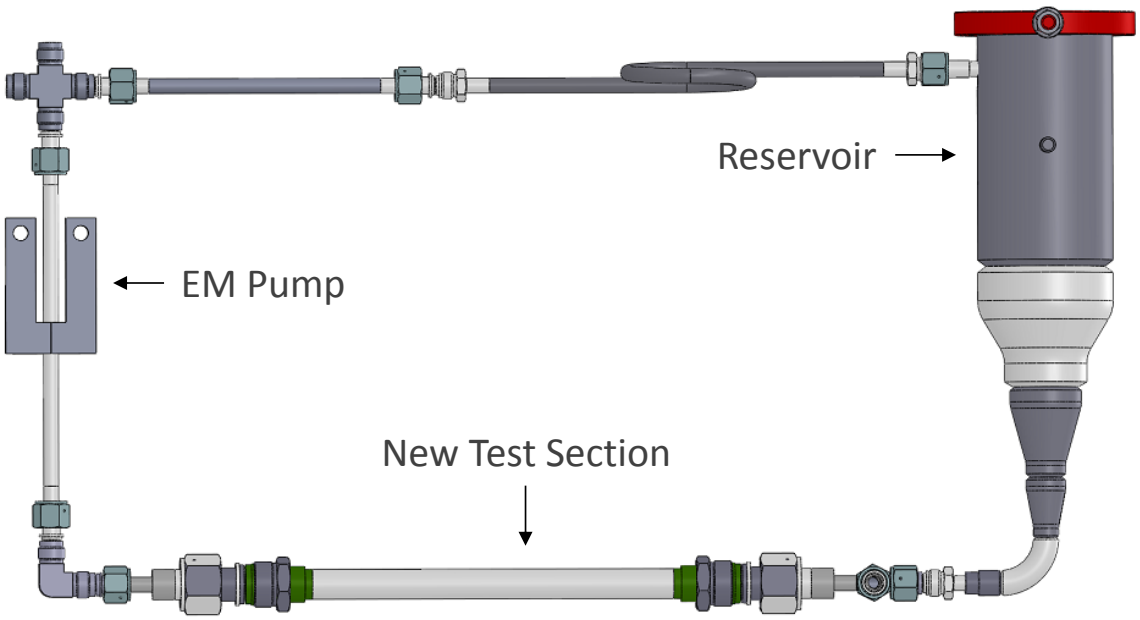

Figure 2. CAD drawing of the upgraded Sodium Freezing and Remelting test facility, not including the cold finger

3.1 Modifications/Upgrades to the Sodium Freezing and Remelting Test Facility

In addition to the upgrading of the freezing and remelting test section to a higher-temperature design, there have been other upgrades/modifications performed to the loop, mainly on the thermocouple instrumentation, EM pump, heating system, electrical connection, and data acquisition system. Shown in Figure 3 is the old Sodium Freezing and Remelting test facility that we started with in FY 2017. Compared to the modified/upgraded test facility shown in Figure 1, it is clearly seen that, the new test facility is much cleaner, neater, and better organized.

Figure 3. The Sodium Freezing and Remelting test facility before modifications/upgrades

3.1.1 Test Section

The new test section differs from the thick-walled 1 inch Schedule 40 pipe test section [5] in the old test facility. Higher-temperature strain gages are implemented on the new test section and the wall is much thinner to enhance the strains achieved. The high-temperature strain gages (model number of HBWAH-12-125-6-3MG-SHB) from Hitec Products, Inc [8] are applicable to temperatures up to 980ºC. The test section is made from 1 inch OD × 0.020 inch thick wall tube of material stainless steel (SS) 316. The overall length of the test section is 16.44 inches, and the fabrication drawing with detailed dimensions is shown in Figure 4.

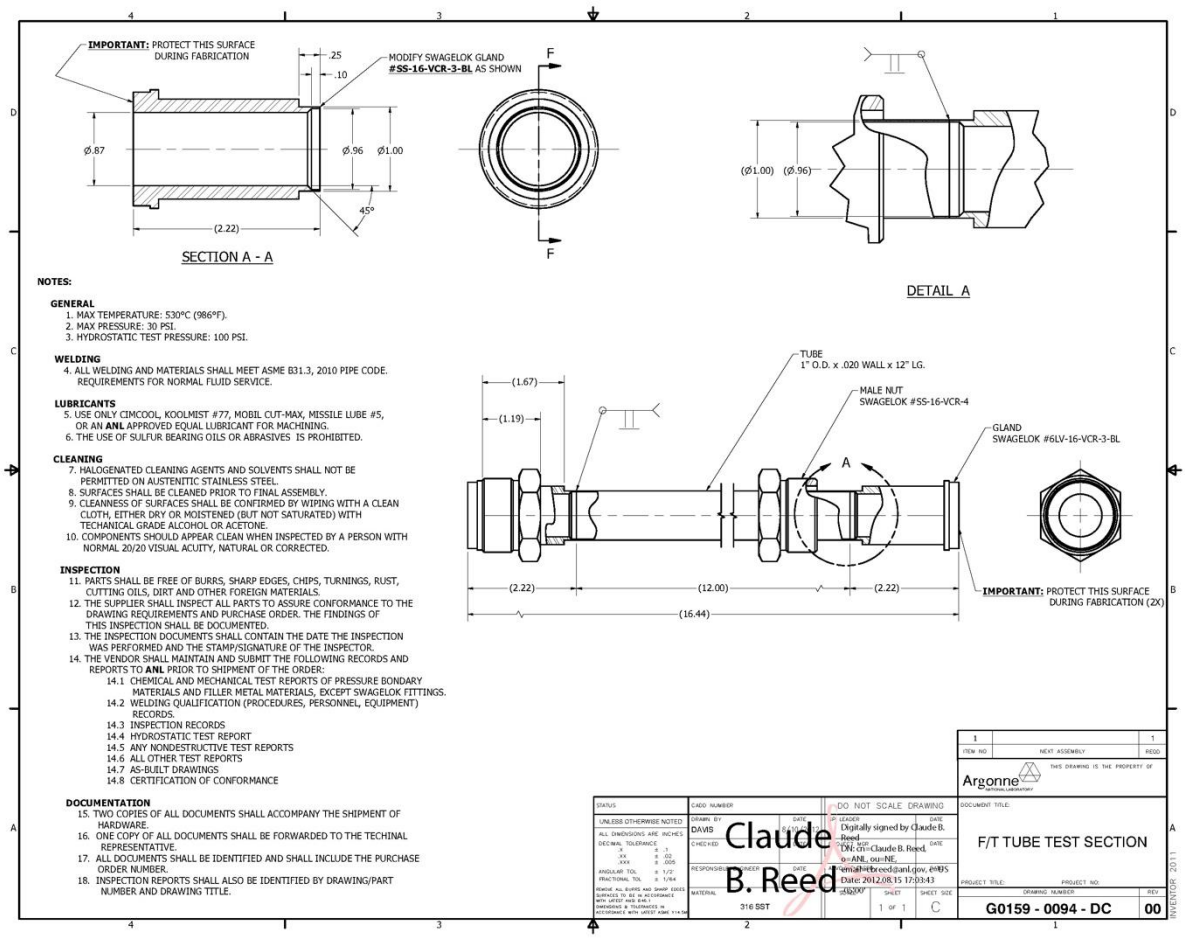

Figure 4. Fabrication drawing of the new test section

The test section has 1 inch VCR fittings welded to each end. Each test section is heavily instrumented on its exterior surfaces with 26 Type K thermocouples and 8 high temperature strain gages. The 26 thermocouples are distributed both axially and circumferentially on the test section's outer surface so that the progression of the freezing or melting front along the length of, and around the circumference of, the test section can be recorded. The 8 strain gages are mounted at three axial locations, -4.8 inch from the center (2), +4.8 inch from the center (2), and the center of test section, and at 0°, 90°, 180°, and 270° around the test section circumference. Four of the eight strain gages are oriented to measure purely axial strain, while the other four strain gages are oriented to measure purely hoop strain. The detailed layout of the 26 thermocouples and 8 strain gages are summarized in Table 1 and Table 2.

Table 1. Detailed layout of the thermocouples on the test section

PART DESCRIPTION: Name	Lead ID	Sensor Description
F/T TUBE TEST SECTION	MINUS 4.8 # 1	0 DRG TYPE- K,SKIN THERMOCOUPLE,.040 DIA,11 FT
	MINUS 4.8 # 2	60 DRG TYPE- K,SKIN THERMOCOUPLE,.040 DIA,11 FT
	MINUS 4.8 # 3	120 DRG TYPE-K ,THERMOCOUPLE .040 DIA, 11FT
	MINUS 4.8 # 4	180 DRG TYPE- K,SKIN THERMOCOUPLE,.040 DIA,11 FT
	MINUS 4.8 # 5	240 DRG TYPE- K,SKIN THERMOCOUPLE,.040 DIA,11 FT
	MINUS 4.8 # 6	300 DRG TYPE-K SKIN THERMOCOUPLE, 040 DIA 11FT
	MINUS 2.4 # 7	0 DRG TYPE- K,SKIN THERMOCOUPLE,.040 DIA,11 FT
	MINUS 2.4 # 8	60 DRG TYPE- K,SKIN THERMOCOUPLE,.040 DIA,11 FT
	MINUS 2.4 # 9	120 DRG TYPE- K,SKIN THERMOCOUPLE,.040 DIA,11 FT
	MINUS 2.4 # 10	180 DRG TYPE- K,SKIN THERMOCOUPLE,.040 DIA,11 FT
	MINUS 2.4 # 11	240 DRG TYPE- K,SKIN THERMOCOUPLE,.040 DIA,11 FT
	MINUS 2.4 # 12	300 DRG TYPE- K,SKIN THERMOCOUPLE,.040 DIA,11 FT
	0 CENTER # 13	0 DRG TYPE- K,SKIN THERMOCOUPLE,.040 DIA,11 FT
	0 CENTER # 14	60 DRG TYPE- K,SKIN THERMOCOUPLE,.040 DIA,11 FT
	0 CENTER # 15	180 DRG TYPE- K,SKIN THERMOCOUPLE,.040 DIA,11 FT
	0 CENTER # 16	240 DRG TYPE- K,SKIN THERMOCOUPLE,.040 DIA,11 FT
	PLUS 2.4 # 17	0 DRG TYPE- K,SKIN THERMOCOUPLE,.040 DIA,11 FT
	PLUS 2.4 # 18	60 DRG TYPE- K,SKIN THERMOCOUPLE,.040 DIA,11 FT
	PLUS 2.4 # 19	120 DRG TYPE-K ,THERMOCOUPLE .040 DIA, 11FT
	PLUS 2.4 # 20	180 DRG TYPE- K,SKIN THERMOCOUPLE,.040 DIA,11 FT
	PLUS 2.4 # 21	240 DRG TYPE- K,SKIN THERMOCOUPLE,.040 DIA,11 FT
	PLUS 2.4 # 22	300 DRG TYPE-K SKIN THERMOCOUPLE, 040 DIA 11FT
	PLUS 4.8 # 23	0 DRG TYPE- K,SKIN THERMOCOUPLE,.040 DIA,11 FT
	PLUS 4.8 # 24	60 DRG TYPE- K,SKIN THERMOCOUPLE,.040 DIA,11 FT
	PLUS 4.8 # 25	180 DRG TYPE- K,SKIN THERMOCOUPLE,.040 DIA,11 FT
	PLUS 4.8 #26	240 DRG TYPE- K,SKIN THERMOCOUPLE,.040 DIA,11 FT

Table 2. Detailed layout of the strain gages on the test section

Part		Sensor ID	Sensor Description
Name	s/n		
ARGONNE	MINUS 4.8	0 DRG AXIAL	HBWAH-12-125-6-3MG-SHB
	MINUS 4.8	180 DRG HOOP	HBWAH-12-125-6-3MG-SHB
	0 DRG CENTER	0 DRG AXIAL	HBWAH-12-125-6-3MG-SHB
	0 DRG CENTER	90 DRG AXIAL	HBWAH-12-125-6-3MG-SHB
	0 DRG CENTER	180 DRG HOOP	HBWAH-12-125-6-3MG-SHB
	0 DRG CENTER	270 DRGHOOP	HBWAH-12-125-6-3MG-SHB
	PLUS 4.8	90 DRG AXIAL	HBWAH-12-125-6-3MG-SHB
	PLUS 4.8	270 DRG HOOP	HBWAH-12-125-6-3MG-SHB

The test section has 1 inch VCR fittings welded on both ends, while the rest of the loop employs ½ inch VCR fittings. To connect the test section to the loop, two reducing connection pieces will be needed. When the work started in FY 2017, although the new test section was already fabricated, it was not finalized on how to connect the test section to the loop. At that time, an initial design using tube coils, as shown in Figure 5, was proposed. It was thought that the tube coils would provide the flexibility to eliminate any external stress from the loop onto the test section. However, calculations were not performed to confirm that thought. In addition, the use of the tube coils would complicate the operation and maintenance (e.g., tilting and draining the loop), as well as inducing increased pressure loss. In view of these considerations, it was decided to perform a study on the flexibility of these tube coils.

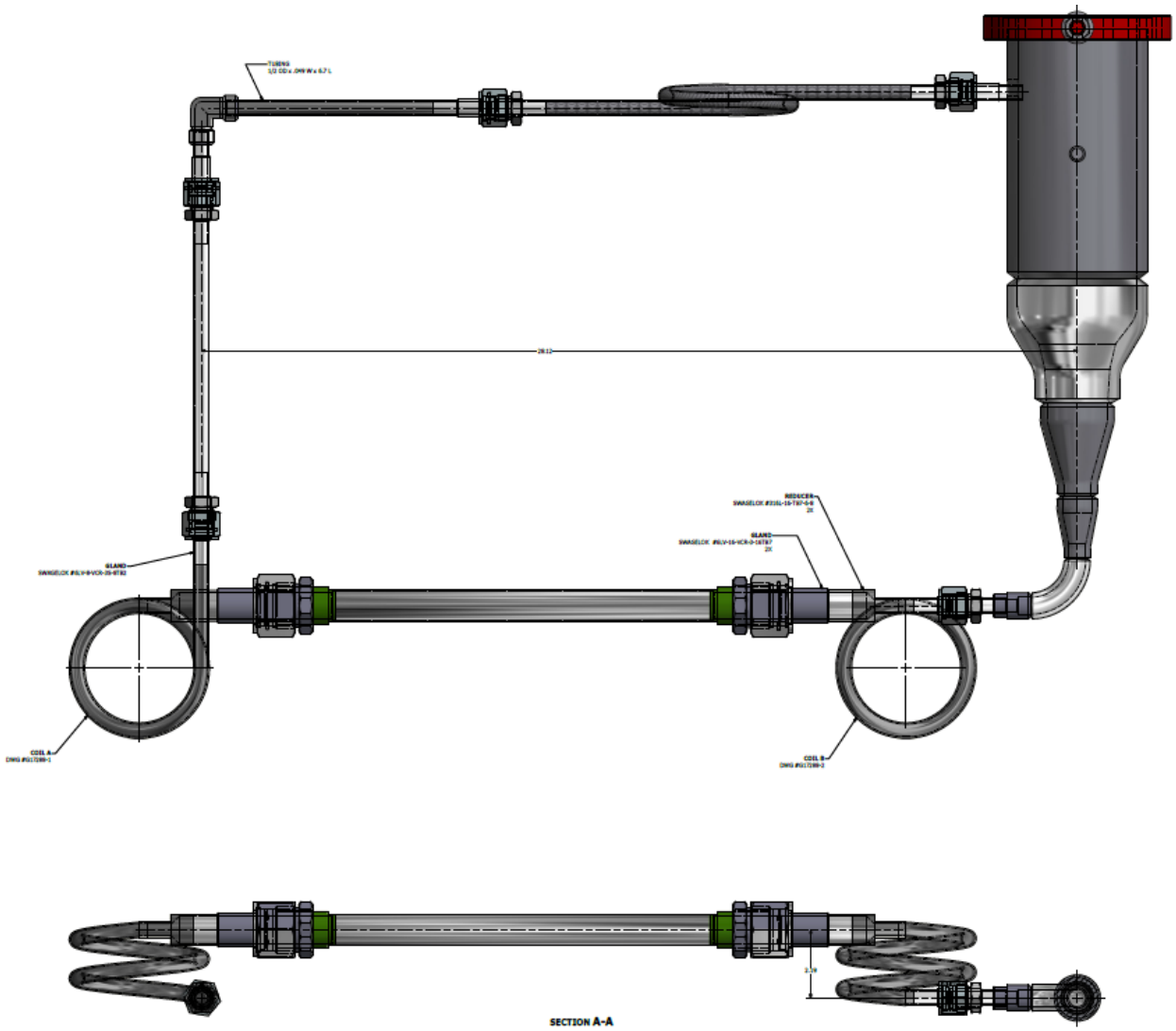

Figure 5. Initial design of connecting the test section to the loop using tube coils

A preliminary study was performed to examine the flexibility of the ½ inch tube coil designed for the new test section in the Sodium Freezing and Remelting test facility. The tube wall is 0.05 inch thick and the coil is 4 inch in diameter (based on tube centerline). The results of the study are summarized as below.

The main purpose of the study was to examine, with the use of the tube coils, how much additional strain will be realized in the test section due to potential non-uniform heating of the loop. The flexibility criterion is that the additional strain caused should be negligible compared to the thermal strain that will be measured directly by the strain gages.

The study was performed in Solidworks using the Simulation package. To simulate the thermal stress, a thermal study is necessary to determine the temperature distribution in the loop. Two cases with different temperature boundary conditions were investigated.

Thermal Study Case 1

In this case, the top center piece is set at 100ºC, and the test section is set at 500ºC. The resulted temperature distribution is shown in Figure 6.

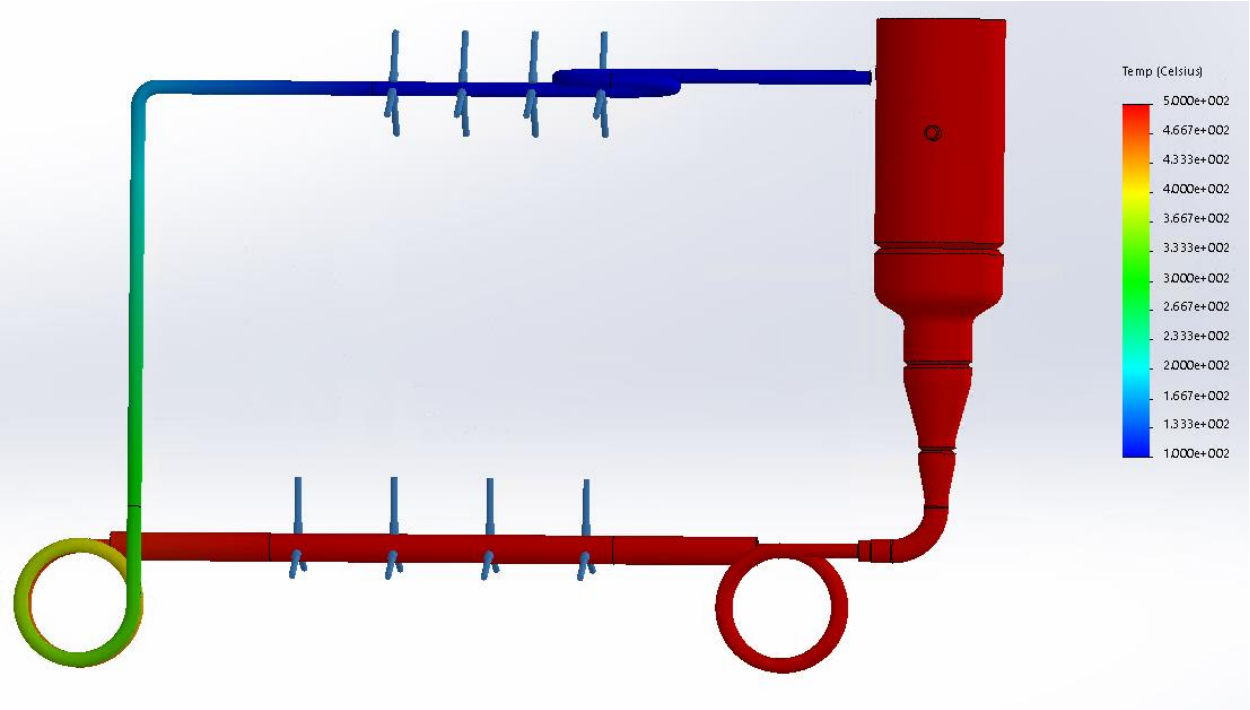

Figure 6. Temperature distribution for thermal study Case 1

Thermal Study Case 2

In this case, in addition to the boundary temperatures applied in Case 1, the top surface of the reservoir is also set at 100ºC. The resulting temperature distribution is shown in Figure 7.

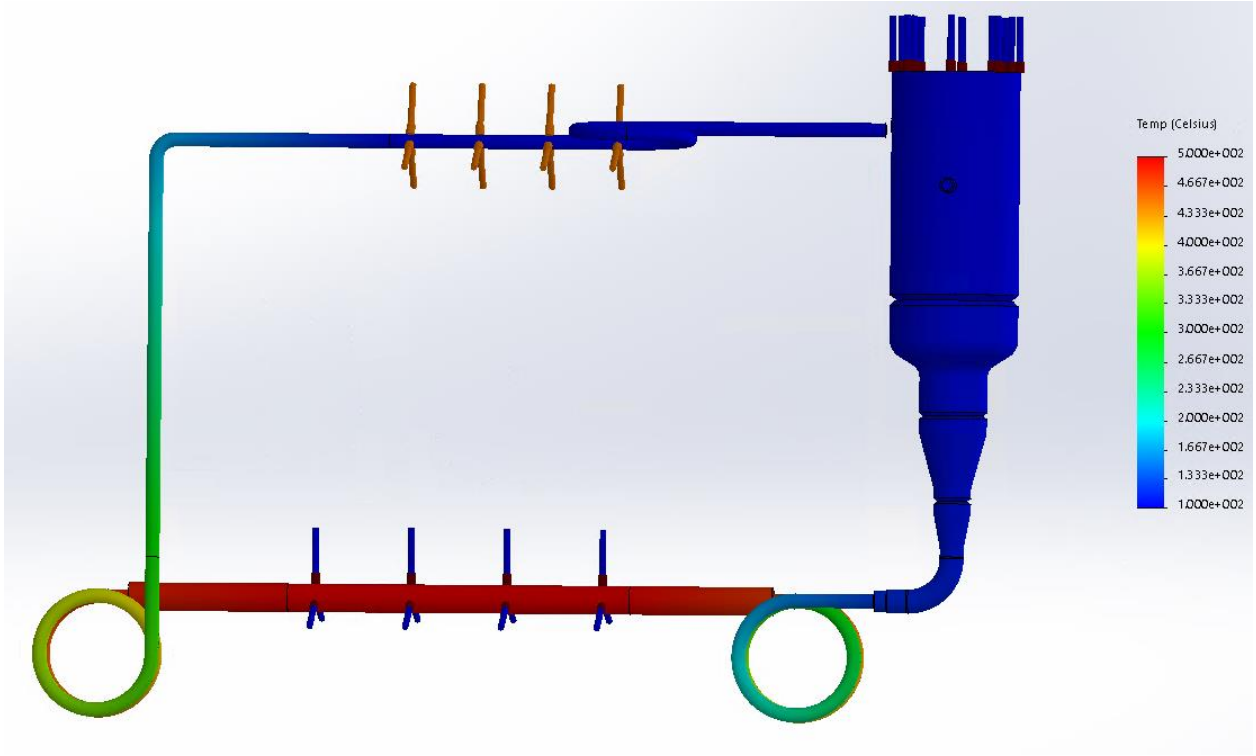

Figure 7. Temperature distribution for thermal study Case 2

With the temperature distribution determined, the thermal stress and additional strain due to non-uniform heating of the loop can be calculated. Four cases of the strain/stress study were performed, with variant loop temperature distributions and fixture boundary conditions.

Strain/Stress Study Case 1

This case adopts the temperature distribution results from thermal study Case 1. In addition, the right end of the top leg and the top surface of the reservoir are fixed, as shown in Figure 8, along with the stress results. The strain results are shown in Figure 9, with a summary of the equivalent strain in the test section shown on the left. As can be seen, the average equivalent strain in the test section is approximately 3.54E-5. Assuming the test section is heated up from 25 to 500ºC and expands freely, the resulting axial thermal strain is approximately 7.60E-3 (assuming a thermal expansion coefficient of 1.5E-5 /K). Therefore, the additional strain accounts only for 0.47% of the thermal strain, and according to the aforementioned criterion, the desired flexibility is ensured. However, based on the deformation of the loop (Figure 8), a significant portion of the flexibility seems due to the loop itself. This issue will be discussed later.

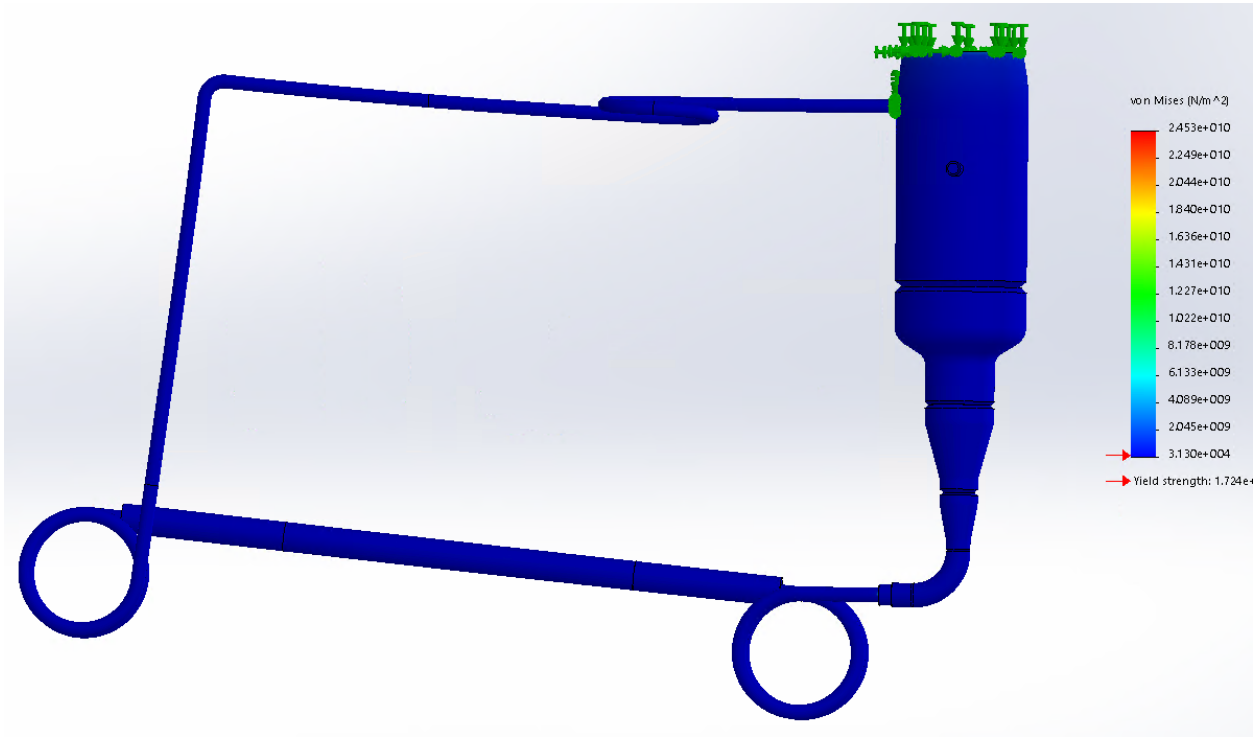

Figure 8. Stress results for Case 1

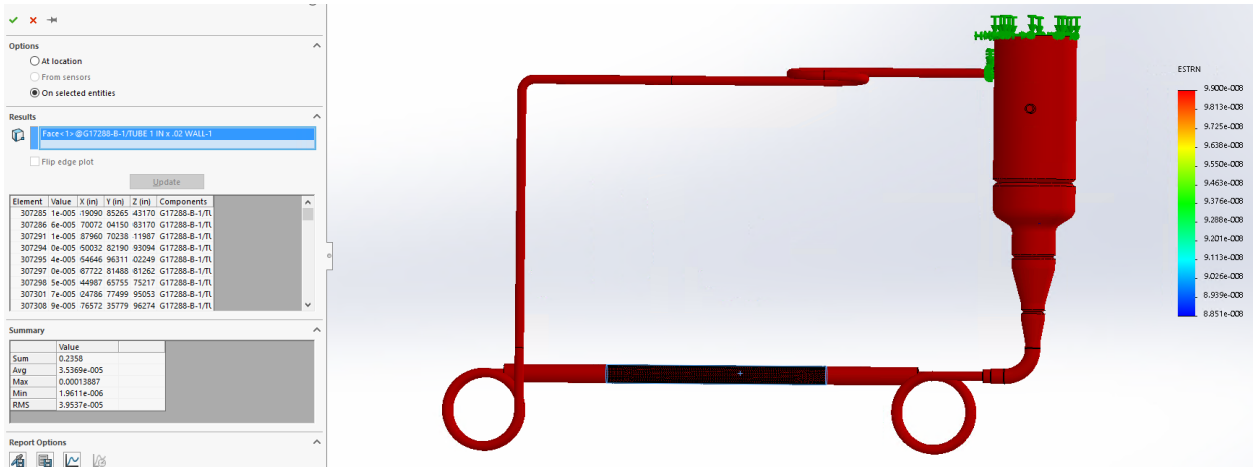

Figure 9. Strain results for Case 1

Strain/Stress Study Case 2

In this case, the same fixture boundary conditions as in the previous case are applied. However, the temperature distribution yielded by thermal study Case 2 is adopted. The stress and strain results are shown in Figure 10 and Figure 11. Again, the additional axial strain induced is negligible compared to the thermal strain.

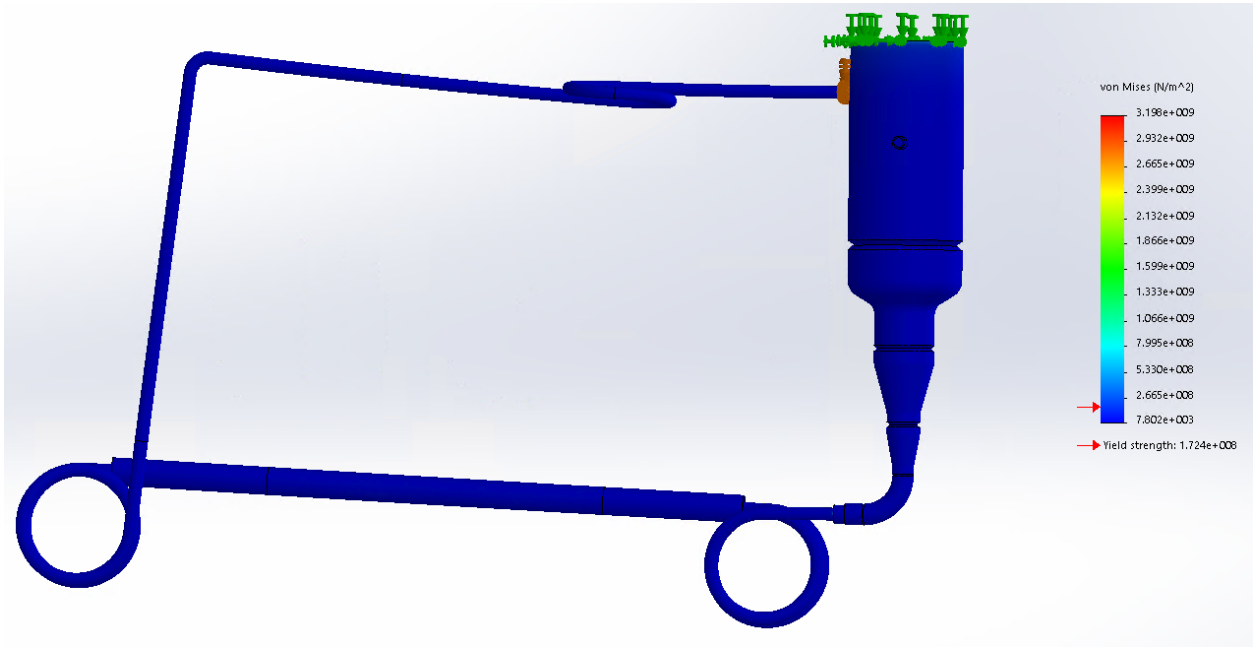

Figure 10. Stress results for Case 2

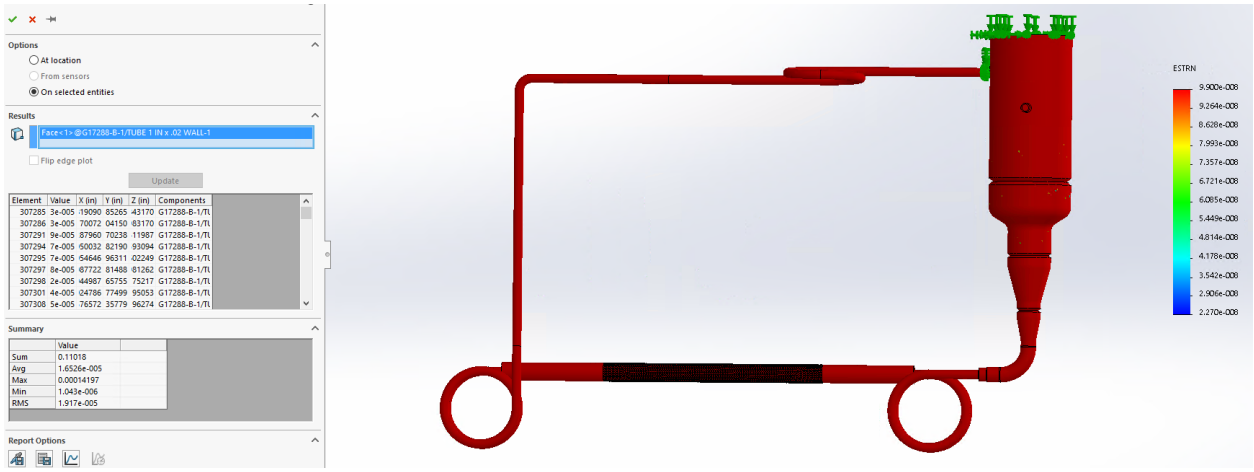

Figure 11. Strain results for Case 2

For the following two cases, the temperature distribution results from thermal study 1 are used.

Strain/Stress Study Case 3

When running the experiments, to maintain good alignment between the magnets and electrodes of the EM pump, it is beneficial to add an anchor point near the EM pump. Therefore, in this case, one additional fixture is added to simulate the anchor. The results are shown in Figure 12 and Figure 13. As can be seen, the additional fixture causes a slight increase in the strain in the test section (compared to case 1), but still negligible compared to the thermal strain.

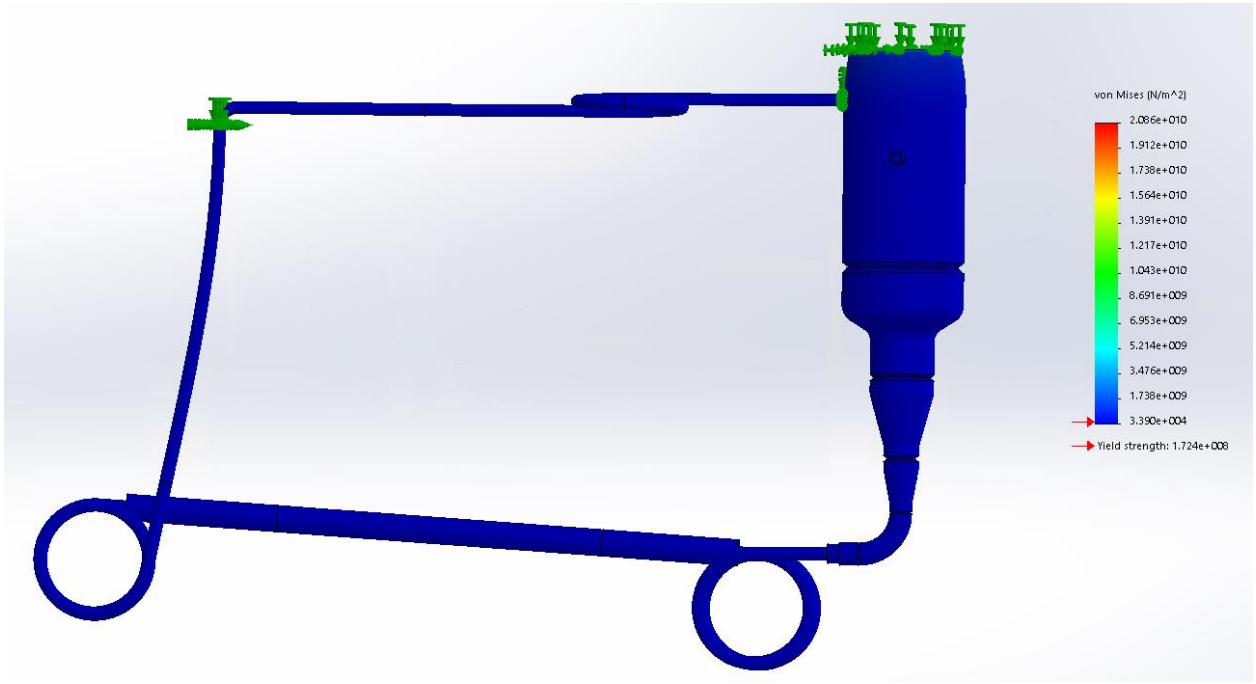

Figure 12. Stress results for Case 3

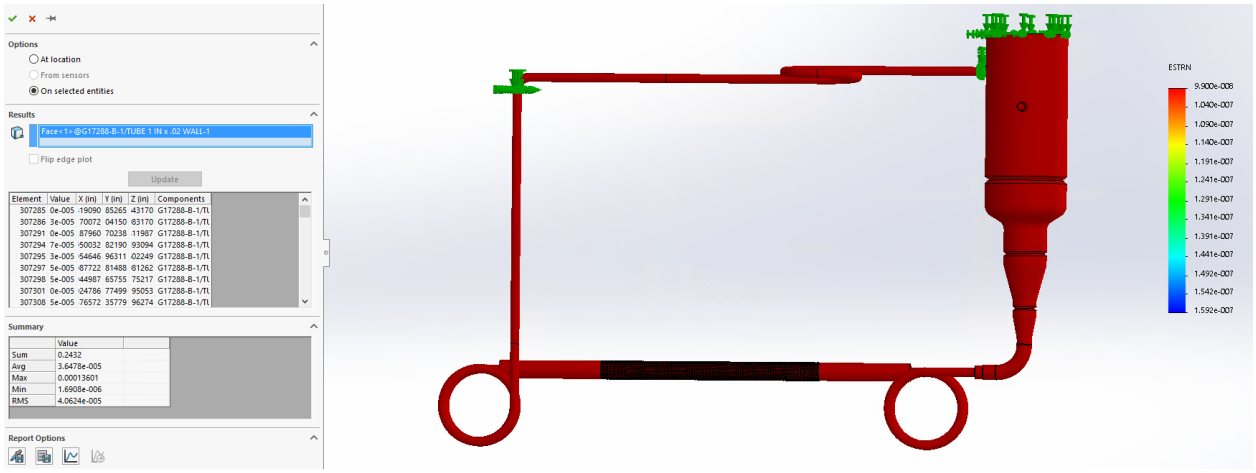

Figure 13. Strain results for Case 3

Strain/Stress Study Case 4

In the last case, the interfaces of the two coils with the loop other than the test section are fixed. The results are shown in Figure 14 and Figure 15. As can be seen, with the two ends of the two coils fixed, significant increases in the stress and strain are caused, indicating that the flexibility observed in the previous cases is greatly due to the loop itself. However, the additional axial strain in the test section now still only accounts for approximately 2% of the thermal strain. This means the coil is flexible enough to avoid causing additional strain in the test section, without assistance from the loop. However, its flexibility compared to that of the loop itself, does not seem to be a significant improvement. In view of this, it was decided to use the simple and straight connection pieces shown in Figure 2, which make the operation and maintenance of the test facility easier.

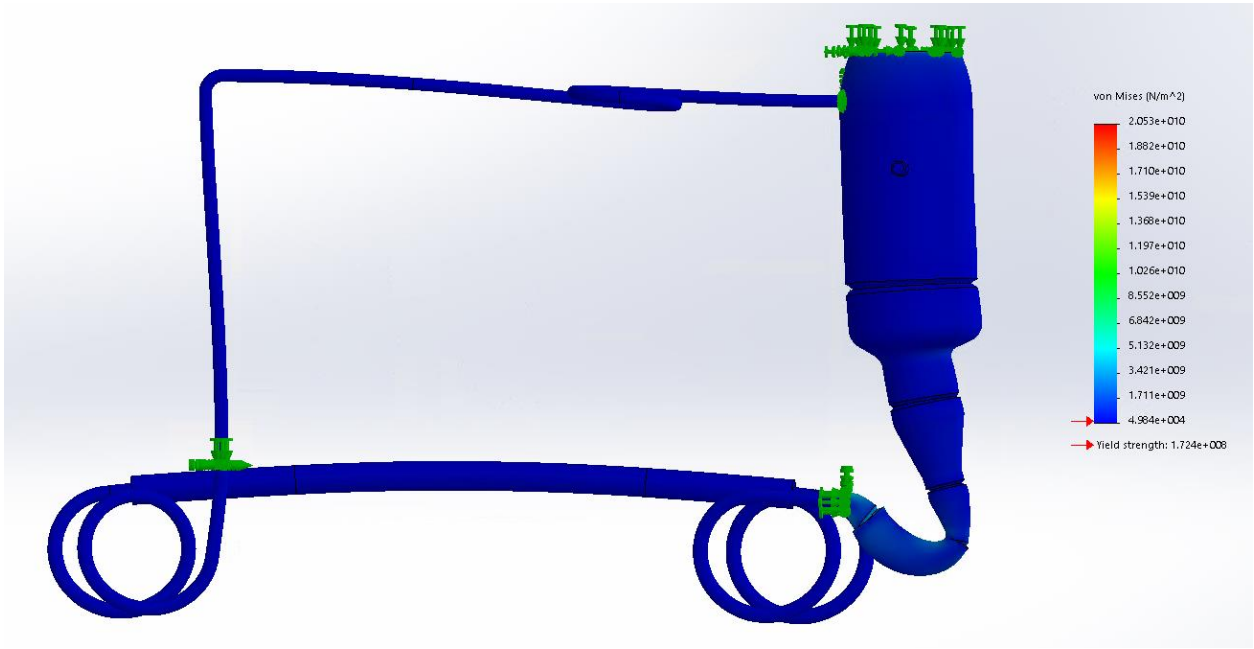

Figure 14. Stress results for Case 4

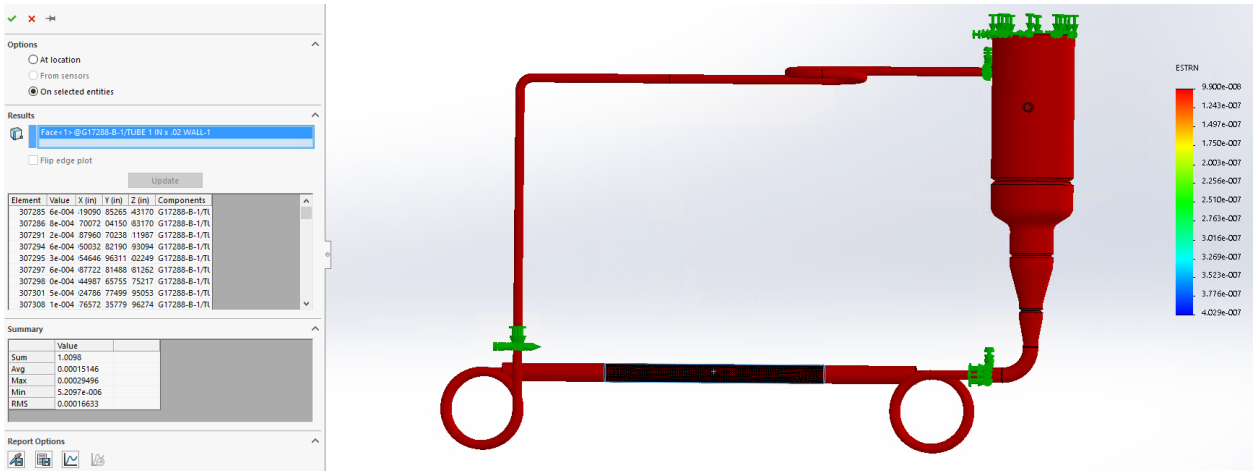

Figure 15. Strain results for Case 4

3.1.2 Electromagnetic (EM) Pump and Power Supply

The EM pump, as shown in Figure 16, is a simple, permanent magnet, DC current-driven, conduction electromagnetic device. The duct is ½ inch × 0.035 inch wall tubing about 13 inches long, with oxygen-free copper electrodes brazed to the outsides of the tube, and then nickel plated to minimize high temperature oxidation of the copper electrodes. Samarium-cobalt permanent magnets are used for their high magnetic field strength, exceptional temperature resistance, and reliable performance without oxidation. The EM pump power supply is an Electronic Measurements, INC. Model 10-1000-2-LB high frequency switching ESS Power Supply providing up to 1000 A at the very low voltage drop across the EM pump electrodes, duct, and sodium inside.

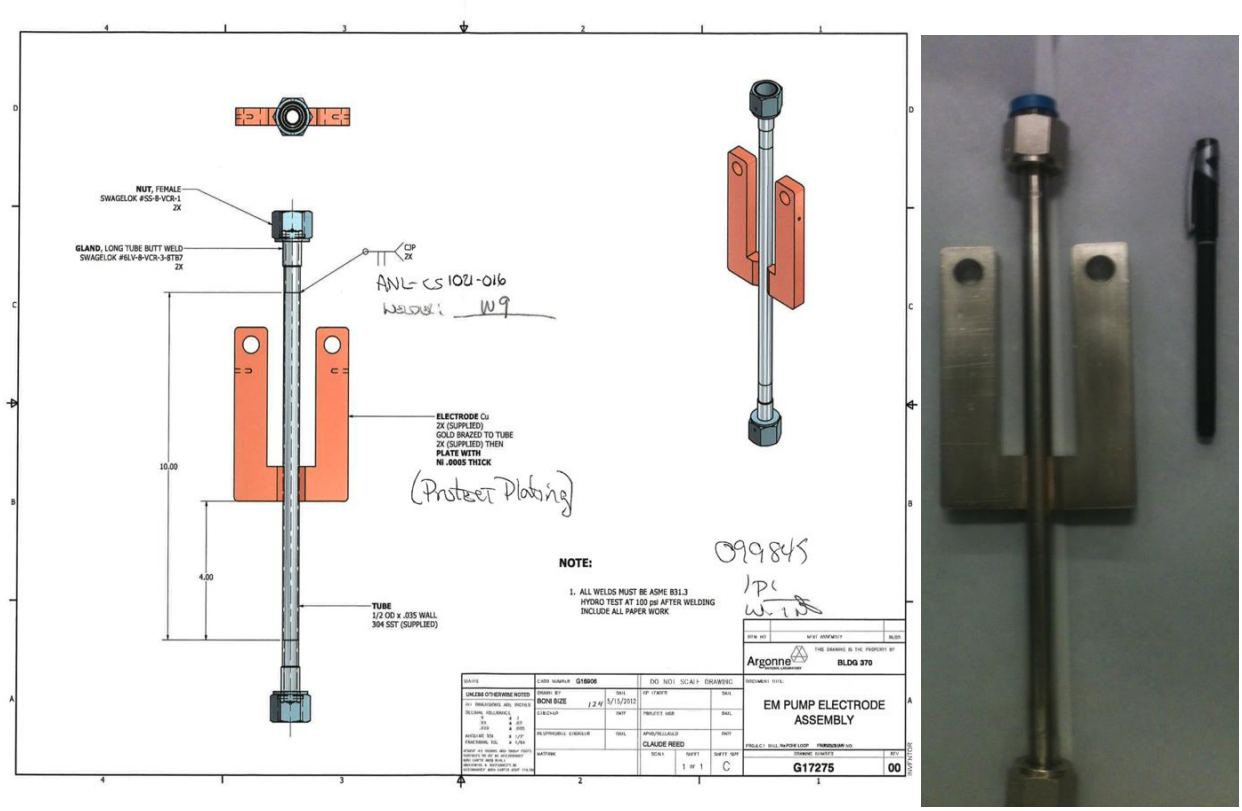

Figure 16. Drawing of EM pump duct and copper electrodes (left), and EM pump duct and electrode assembly after nickel plating

Two improvements were made to the EM pump. First, in the old test facility, the EM pump was installed in a way that the electrode plane was perpendicular to the loop plain. The issue with this EM pump orientation is that when the loop is heated and thermally expands, the EM pump duct and electrodes will contact the magnets that are fixed, causing external stress on the loop as well as a potential electrical short. Therefore, when the test facility was reassembled, we decided to rotate the EM pump by 90º, so that the pump duct along with the electrodes can move freely in the gap between the two magnets when the loop thermally expands, as shown in Figure 17. In addition, as may be noticed, the EM pump duct is not positioned exactly at the centerline of the magnet set, but slightly toward the right as shown in Figure 17. This intentional misalignment was to account for the thermal expansion of the loop when heated. Second, in the old test facility, a thin layer of mica sheet was attached to the magnet surfaces to provide the necessary electrical insulation between the electrodes and magnets. This was not deemed as a reliable design. The mica sheets were replaced with thicker ceramic fiber sheets that were fixed to the magnets with steel wires, as shown in Figure 17. The thicker ceramic fiber sheets provide not only the necessary electrical insulation but also good thermal insulation.

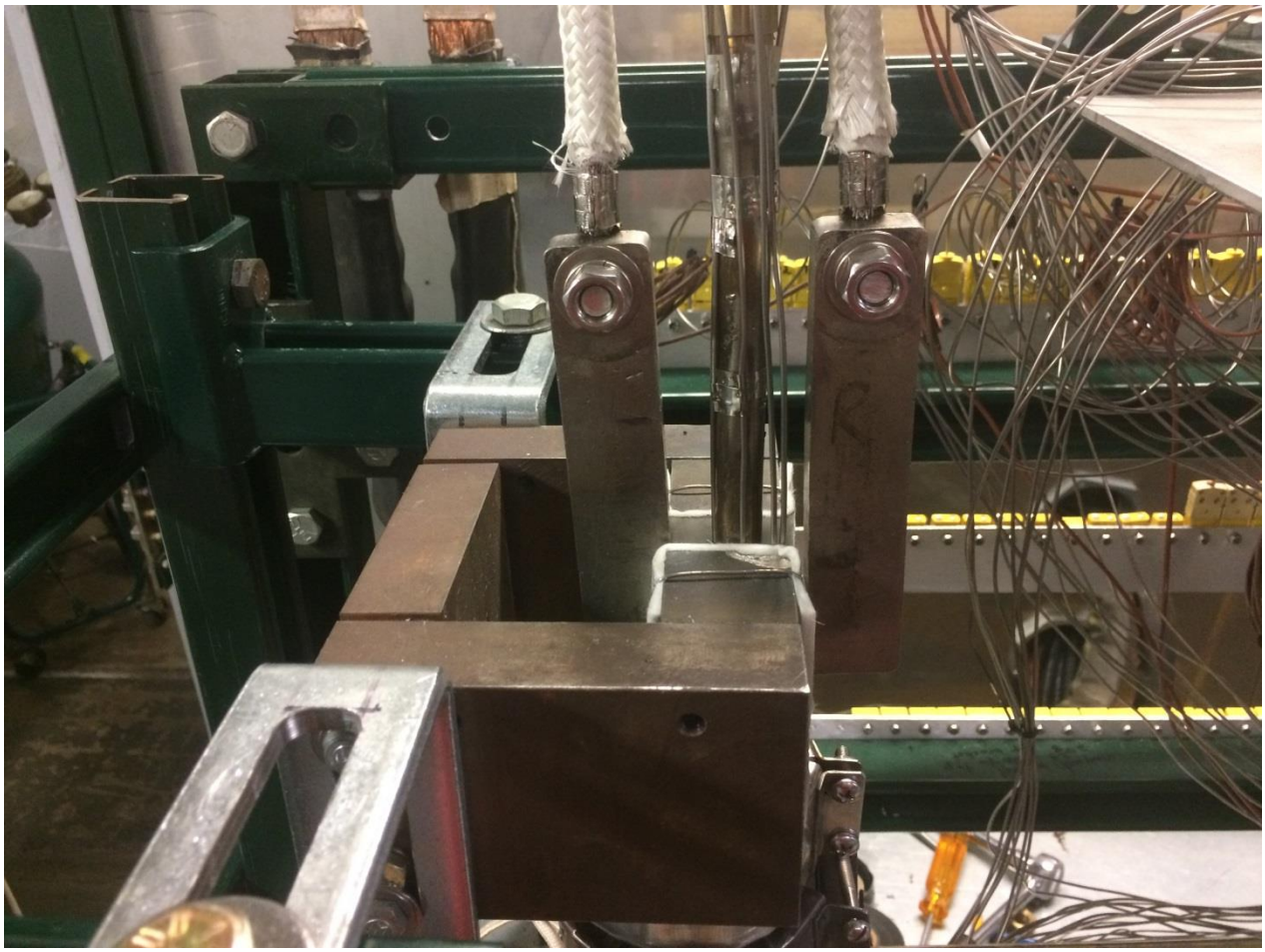

Figure 17. Picture showing the orientation of the EM pump

3.1.3 Heating System

Twelve (12) separate, independent heating zones are implemented to properly and flexibly melt and freeze the apparatus and test section. Ceramic band heaters, as shown in Figure 18, are used for heating zones. One of the modifications to the test facility was on the heating of the EM pump. Previously, the pump duct above the magnets was heated with mica insulated contact heaters, and the electrodes were heated with ceramic strip heaters. In the new test loop, all those heaters were removed and replaced with large diameter ceramic band heaters encompassing both the pump duct and electrodes for heating. Heating or cooling is controlled for each zone by its own independent proportional-integral-difference (PID) controller. A separate, independent temperature limit controller is also provided for each zone. A photo of the Zones 1-6 front panel is shown in Figure 19.

The heating zones had to be modified mainly due to the modification to the test section. Also, as mentioned above, heating of the EM pump region was modified, thus requiring the modification of the corresponding heating zone. A map of the new heat zones is shown in Figure 20.

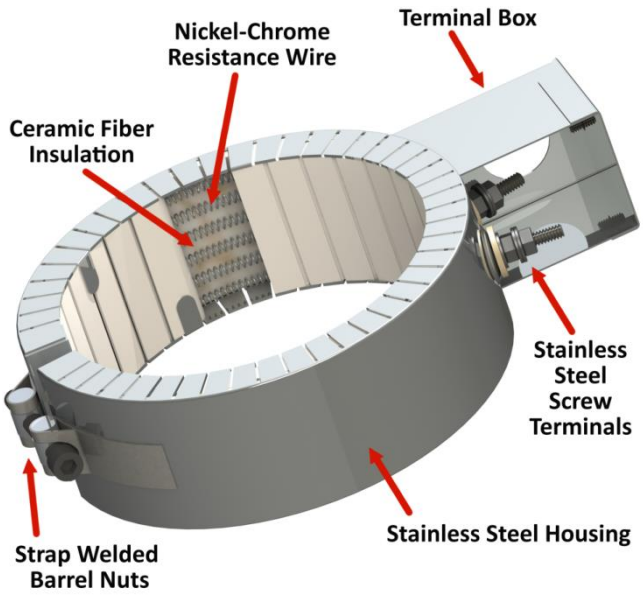

Figure 18. Ceramic band heaters

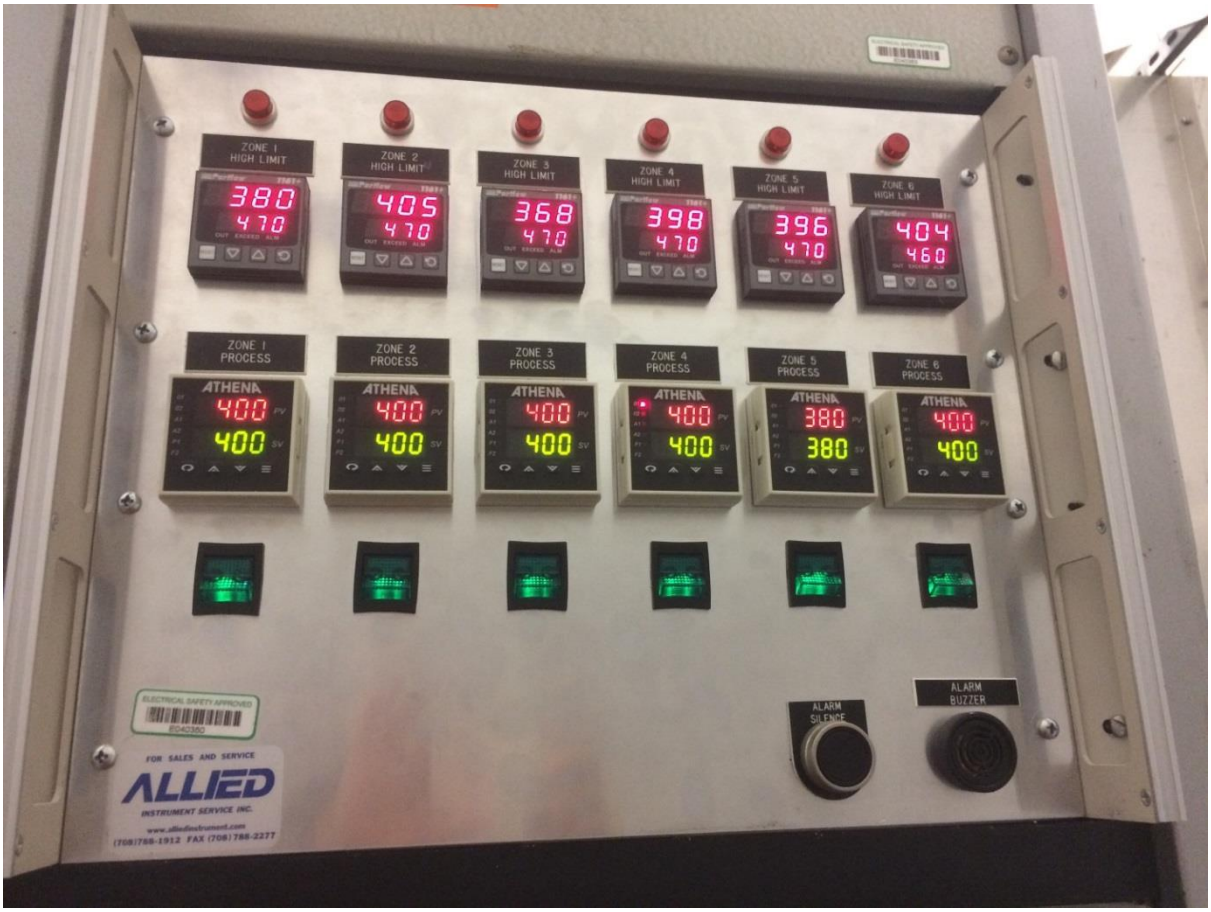

Figure 19. Front panel of heater control system for Zones 1-6 (picture taken during the ~ 400ºC test performed in FY 2017)

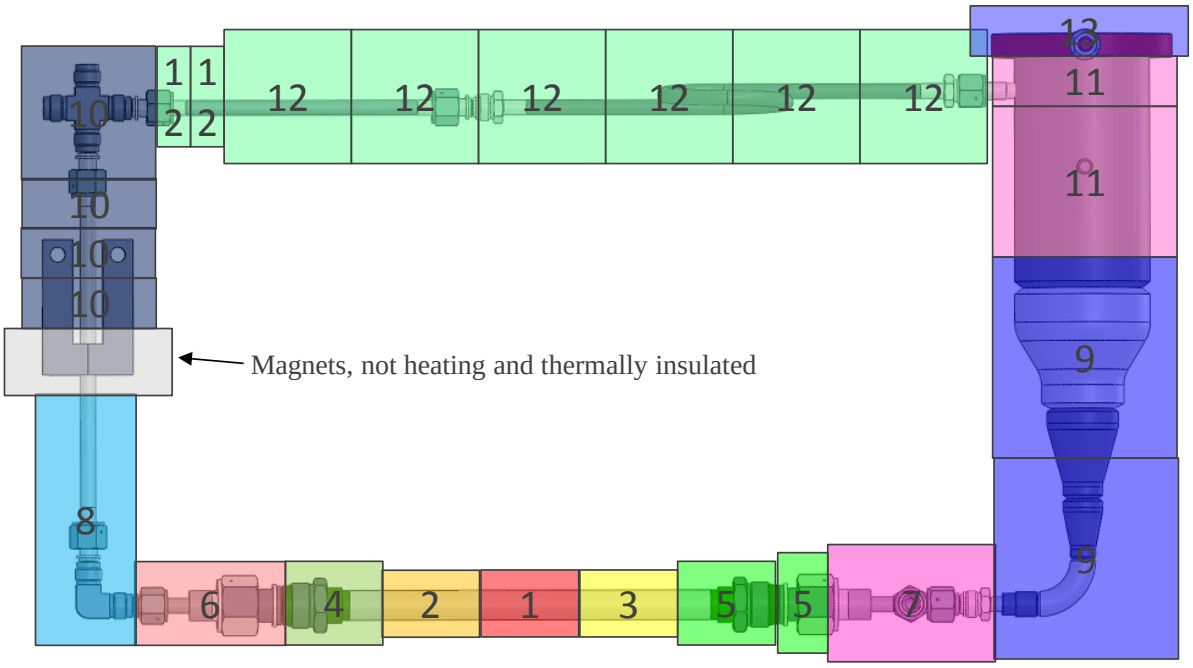

Figure 20. Updated heating zones for the Freezing and Remelting test facility

3.1.4 Thermocouple Instrumentation

When disassembling the old test facility, to facilitate the process, most of the old thermocouples were removed. After the reassembly was completed, new thermocouple instrumentation was designed and implemented. A total of 112 Type K thermocouples were installed in the new Freezing and Remelting test facility. Among these 112 thermocouples, 26 are located at the test section, as discussed earlier. There are 40 thermocouples used to measure the loop temperatures, among which 32 thermocouples are welded to the surface of the loop, 6 are inserted into the loop, and 2 are used to monitor the magnet temperature. There are 24 thermocouples connected to the power control system, 12 for PID temperature controllers and the other 12 for temperature limit controllers. The remaining 22 thermocouples are inserted into the leak detecting holes of all the VCR fittings (2 holes per VCR connection) to monitor for sodium leakage. These thermocouples are connected to a PLC warning system, and whenever a leak is detected, the system will immediately notify the personnel in charge so that proper actions can be taken in time. The approximate layout of all the instrumented thermocouples can be found in Figure 21

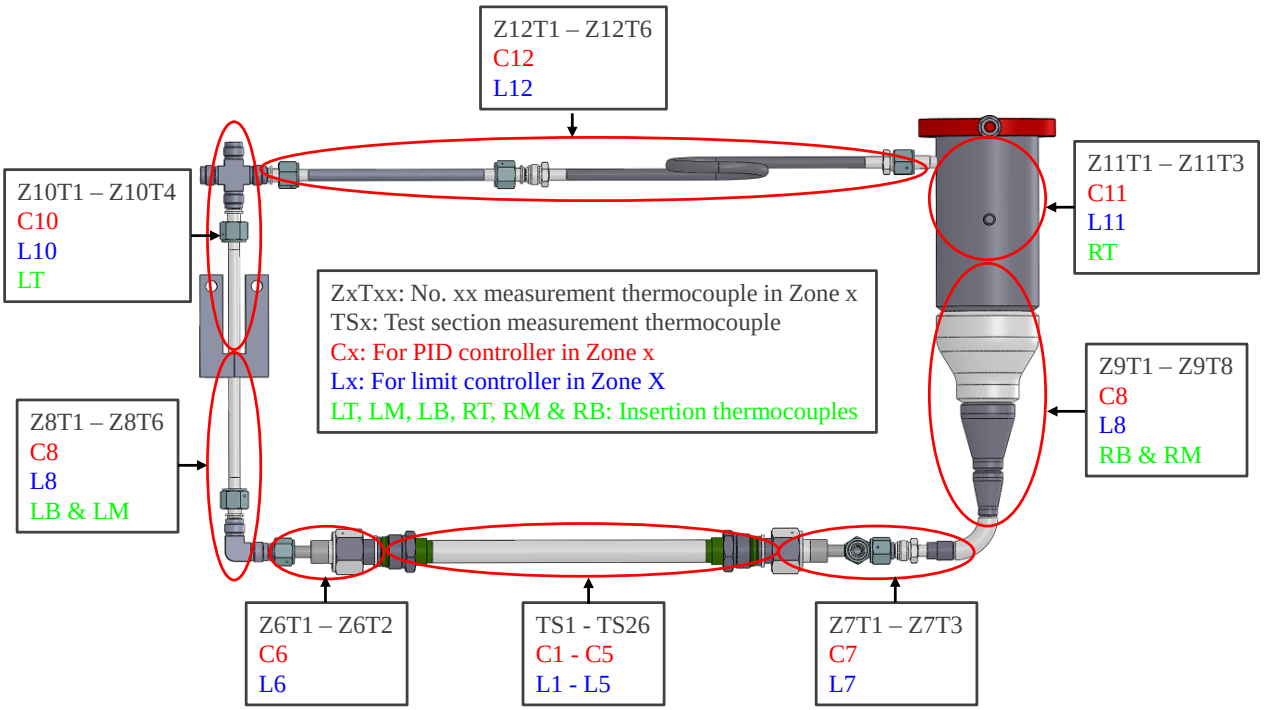

Figure 21. Layout of the instrumented thermocouples

3.1.5 Data Acquisition System

For the old Freezing and Remelting test facility, the data acquisition system consisted of an Agilent Technologies 34970A Data Acquisition Unit and a Vishay Micro-Measurements System 5000, Model 5100B Scanner. The Agilent system was used to acquire data on temperatures, test facility loop pressure, EM pump supply voltage and current, and test section voltage drop. The Vishay system was used to record the strain data for the 8 strain gages on the test section. The whole data acquisition system ran on a Windows XP PC. There was an attempt to migrate the data acquisition system from the old Windows XP PC to a newer Windows 7 PC, which will enable remote monitoring and controlling of the loop operation. However, it was found that the Vishay scanner would not support the Windows 7 operating system. Therefore, a newer Vishay scanner, Model 8000 was purchased. The new strain scanner is more compact, faster, and works well with the Windows 7 system.

3.1.6 Electrical Connection

The Sodium Freezing and Remelting test facility is located inside an isolated enclosure cell, while the heating power supply and control system is located outside of that cell for heat shielding purpose. In the old test facility, the heater wires were connected to the power supply and control system through terminal blocks that were only covered with plastic covers and not well shielded. This was considered not safe, and it was decided to install an electrical enclosure to house the terminal blocks for better electrical shielding. A picture showing the installed electrical enclosure can be found in Figure 22.

Figure 22. Installed electrical enclosure for better electrical shielding

3.2 Sodium Reservoir

One of the components that was not modified during the upgrade of the Freezing and Remelting test facility is the sodium reservoir. Figure 23 shows a cross section of the reservoir and sections of each reservoir subcomponent beside a photo of the as-fabricated reservoir. The sodium reservoir serves mainly four purposes. First, sodium is initially loaded and subsequently added through the sodium reservoir. Second, the Freezing and Remelting test facility is not completely filled with sodium and there is some open space at the top of the reservoir. The test facility can be vacuumed or pressurized through the reservoir. Third, the reservoir houses the cold finger that will collect impurities when the sodium is in circulation and the cold finger is cooled with air. Last, when the test section or any other component in the test facility is to be removed, the sodium is drained into the reservoir by simply rotating the apparatus ninety degrees so that the reservoir is the lowermost component of the apparatus. The reservoir size (2 liters) as well as the volumes of the other components was sized so that the test section completely drains into the large reservoir when the apparatus is rotated, yet adequate sodium covers the EM pump electrodes when the test facility is back to its normal orientation.

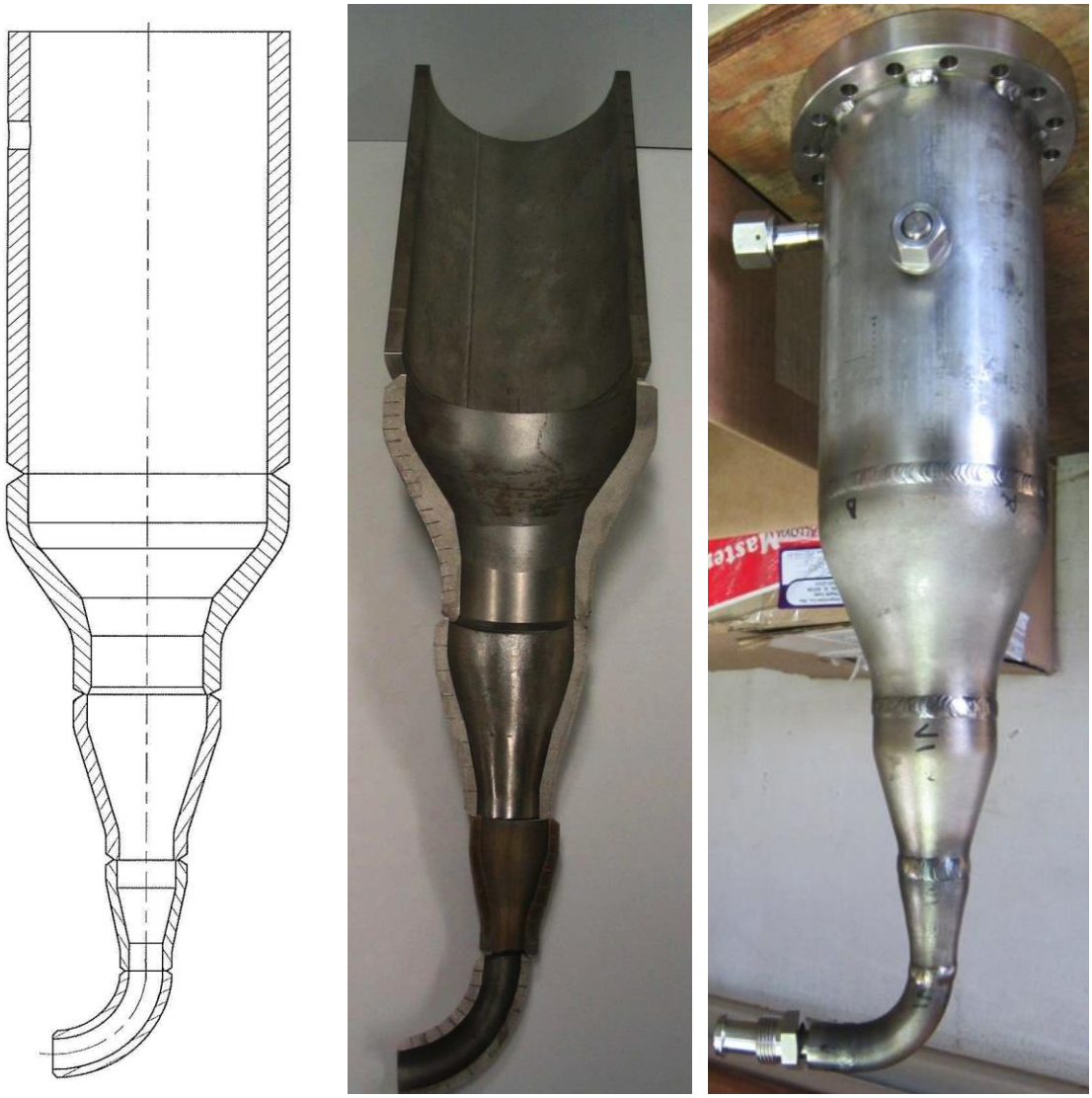

Figure 23. Section View (Left), Sectioned Duplicates of Components Comprising the Sodium Fill Reservoir (Center) and Fabricated Reservoir (Right)

3.3 Cold Finger

Liquids will break apart, or form voids, under sufficient tension. Literature review [9] showed that several factors can play a role, including temperature, degree of impurity, amount of dissolved gases, geometry, surface conditions of surrounding structures, ionizing radiation, and frequency. In the case of sodium, some of these factors, such as degree of impurity, amount of dissolved gases, surface conditions of surrounding structures, can be lumped together under the concept of wetting. In the original design of the Sodium Freezing and Remelting test facility [5], the cold finger was not part of the design. To add a sodium purification capability to the Freezing and Remelting test facility, a simple air-cooled cold finger was designed and fabricated [7] for insertion into the sodium reservoir by replacing the existing flange with a newly fabricated flange, see Figure 24 - Figure 29. In operation, air is forced down a tube that is inside and concentric with the cold finger outer tube; the air then returns along the annulus, removing heat and lowering

the temperature of the cold finger tube, thereby creating the coldest sodium-wetted surface inside the Freezing and Remelting test facility. After circulating the sodium for some time inside the Freezing and Remelting test facility while operating the cold finger, the main impurity in the sodium, oxygen, will be collected on the outer surface of the cold finger, thus purifying the sodium. The facility does not incorporate a sodium plugging meter or any other capability to actually determine the oxygen impurity level.

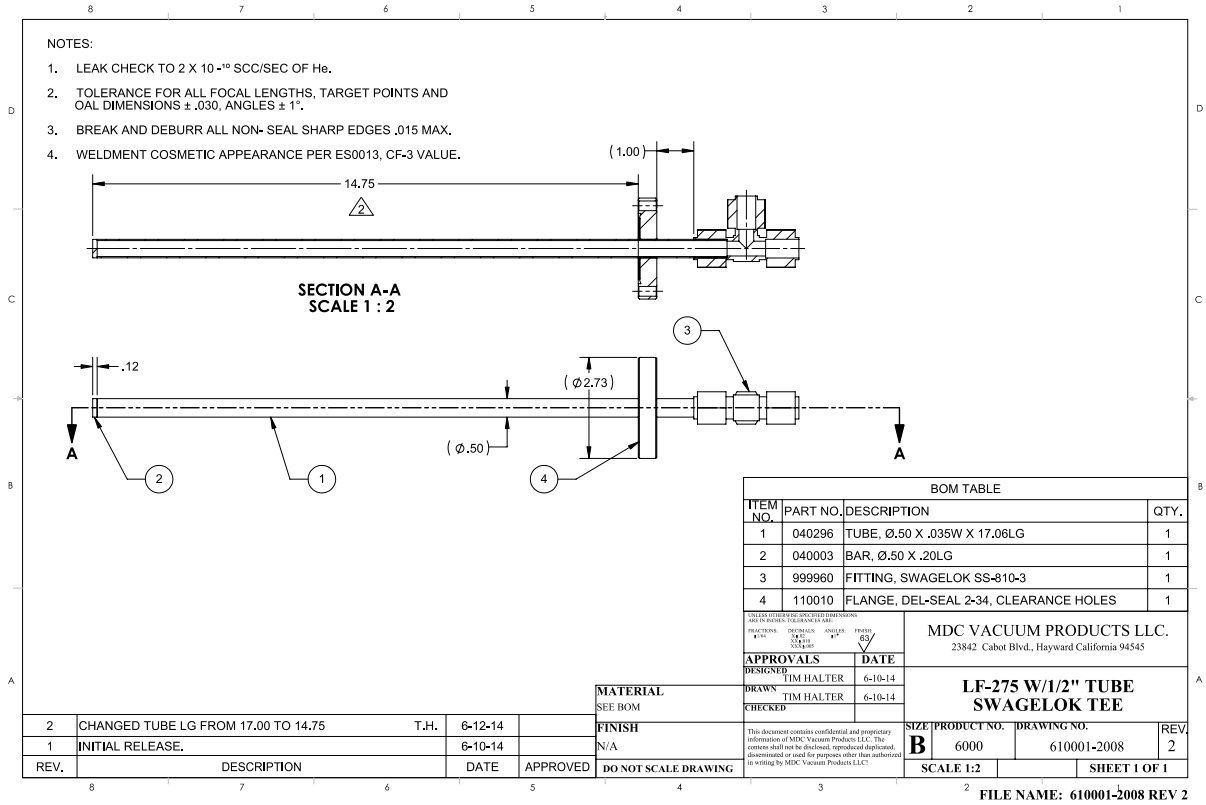

Figure 24. Cold finger fabrication drawing

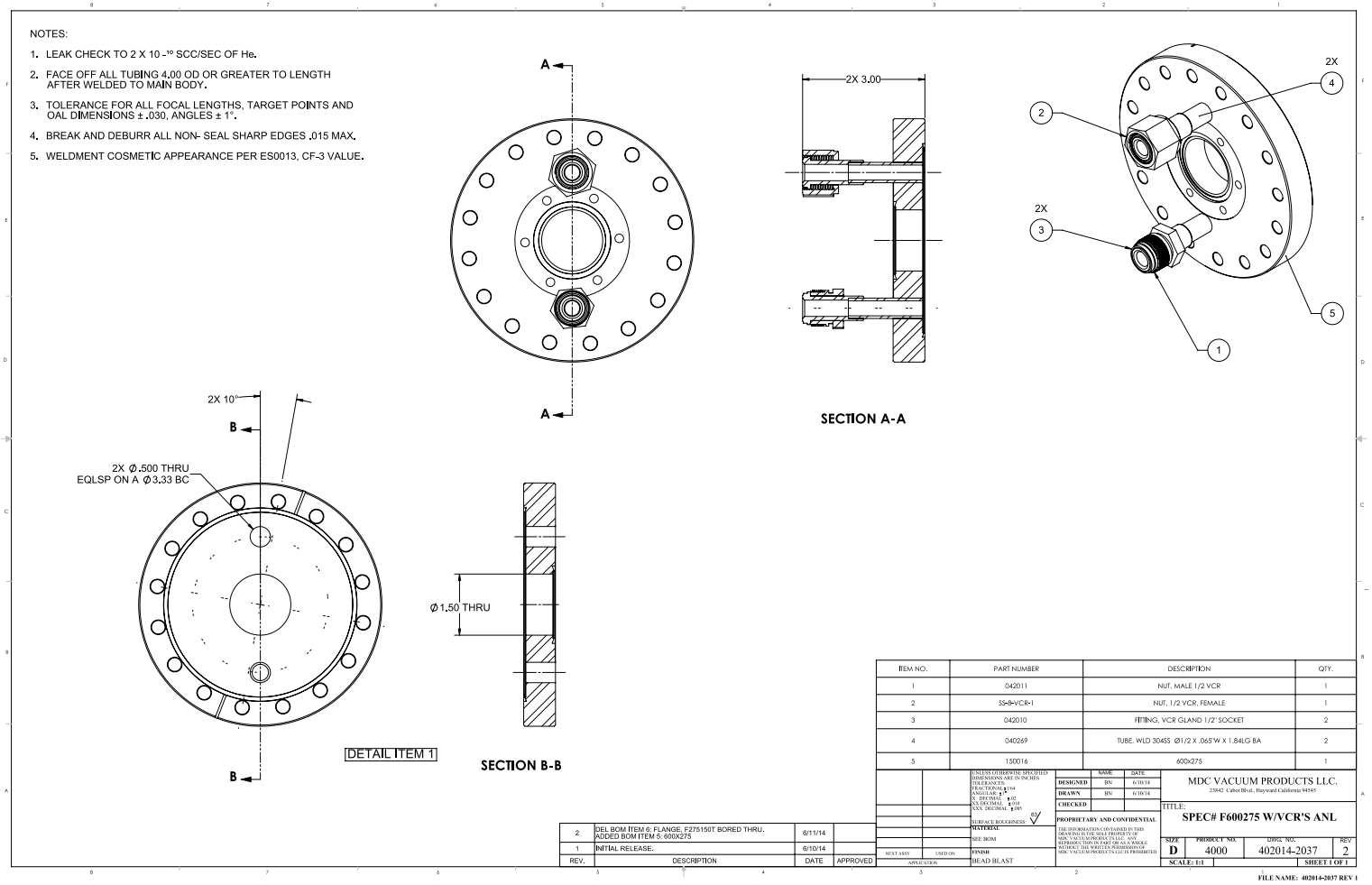

Figure 25. Cold finger top flange

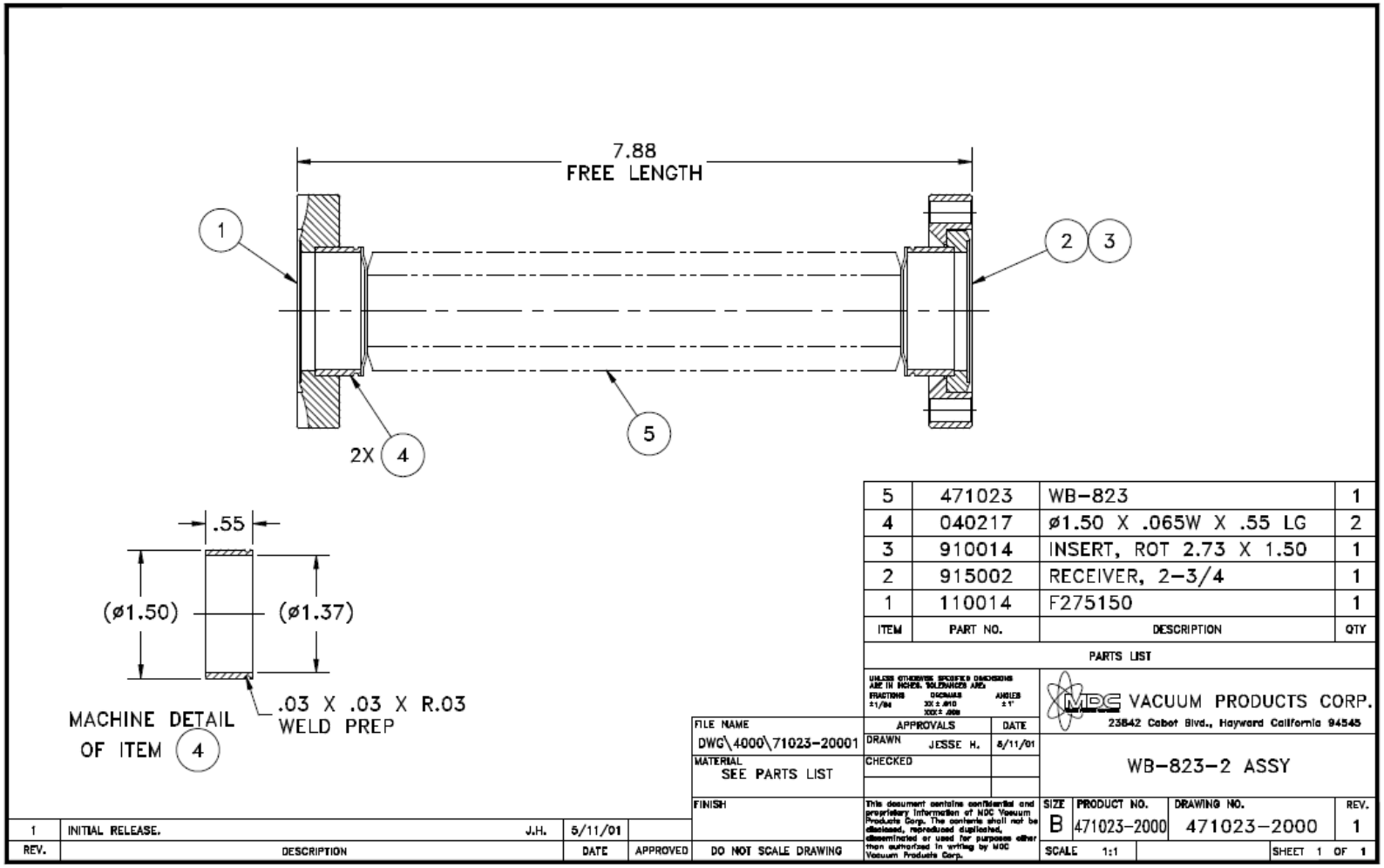

Figure 26. Cold finger bellows drawing

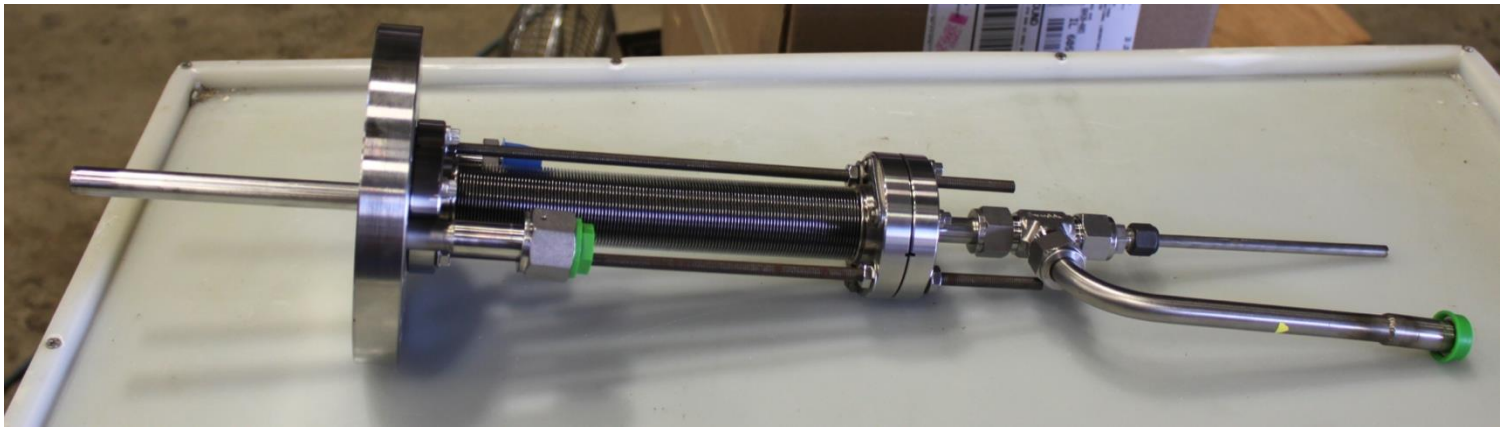

Figure 27. Cold finger assembly

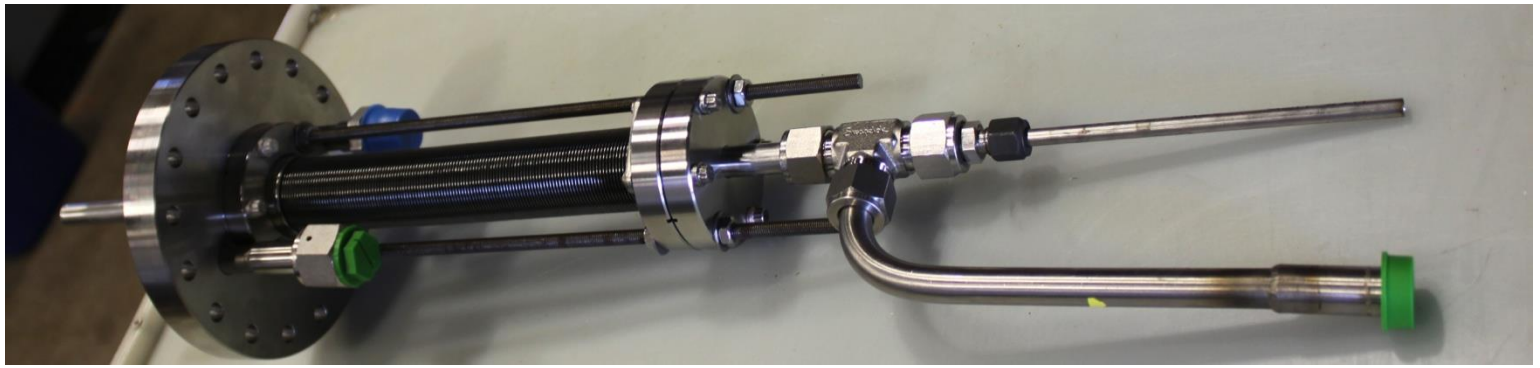

Figure 28. Cold finger top view

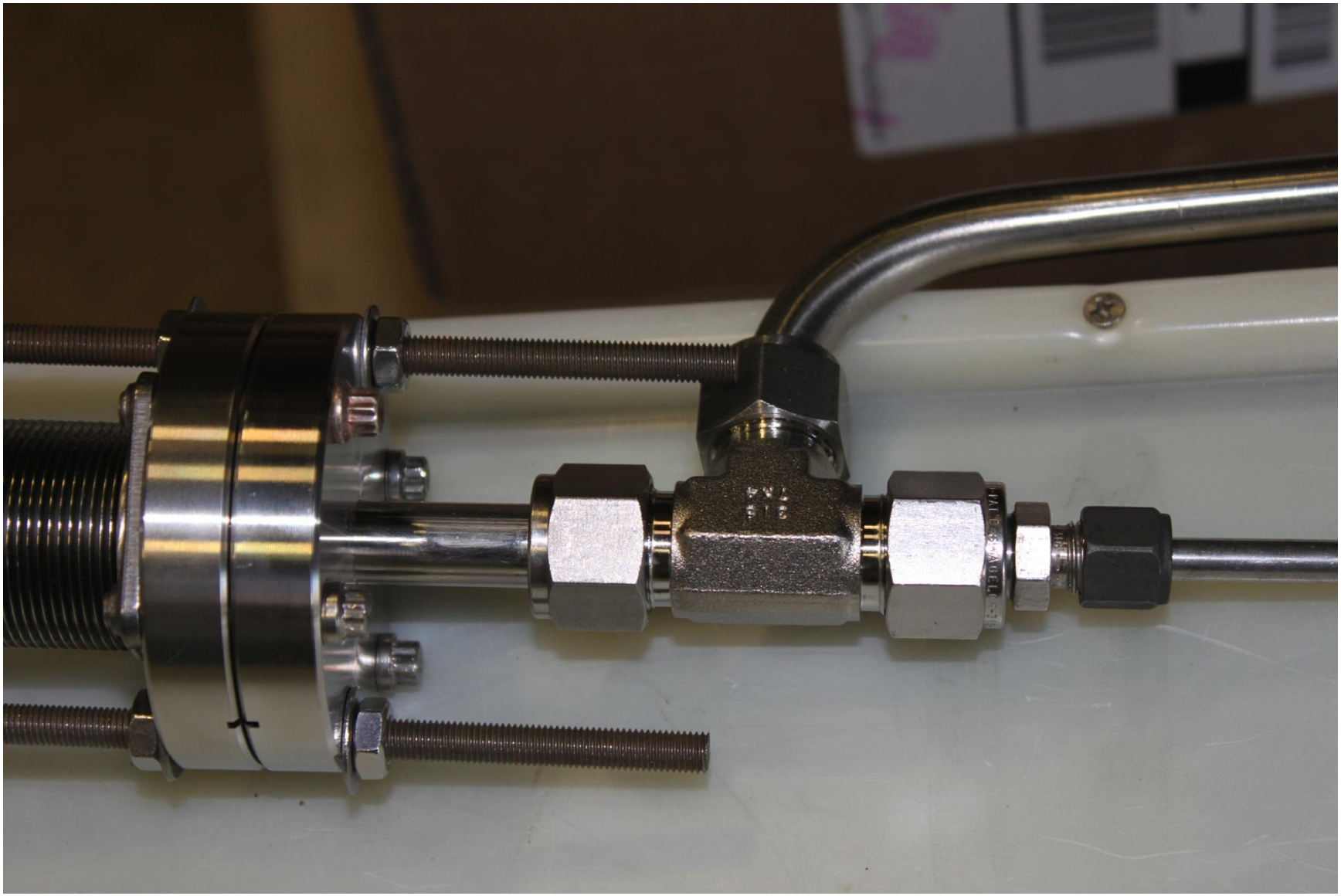

Figure 29. Cold finger air inlet/outlet

4 Baseline Tests

A series of baseline tests on the new test section, including pressure response tests, temperature response tests, and strain gage balance tests were performed before and after the new test section installation. These tests would provide useful baseline data for correction and troubleshooting that may be needed for subsequent formal tests.

4.1 Strain Gage Balance Test

Before the new test section was shipped to Argonne, the vendor performed a balance test on the 8 strain gages, where the test section was free to external stresses. Similar tests were performed on site at Argonne to double check the test data provided by vendor, as well as to acquire the baseline data that may be needed for future tests. Both pre-installation balance testing where the test section was free from external stresses and post-installation balance testing where the test section might be subject to external stresses due to the rest of the loop were performed. The test results, along with the test data from vendor, are summarized in Table 3.

Table 3. Strain gage balance test results

Sensor ID	Sensor Location	Sensor Info	Vendor Data, με	On-Site Test Results, με	
				Pre-installation	Post-installation
7	-4.8”	0º Axial	1712	1772	1731
8	-4.8”	180º Hoop	-660	-947	19
3	Center	0º Axial	-1266	-2165	-2179
4	Center	90º Axial	-70	-92	-159
5	Center	180º Hoop	138	425	111
6	Center	270º Hoop	-658	-1069	-870
1	+4.8”	90º Axial	-882	-777	-567
2	+4.8”	270º Hoop	362	278	494

4.2 Strain Gage Pressure Response Test

This test was performed to check the response of the strain gages to the internal pressure inside the test section. Pressurized water was used for this test due to safety concerns (to reduce the stored energy). For this test, the test section internal pressure was increased from atmospheric pressure to ~ 500 psig. All the strain gages were zeroed at atmospheric pressure before the test section internal pressure was increased. The test results are plotted in Figure 30. As can be seen, the response of the strain gages to the test section internal pressure is quite linear, indicating that the test stays in the elastic regime. Also, the strain readings separate themselves into roughly two groups, except for the outlier of Gage 6 reading. The hoop strains are much larger than the axial strains, which is understandable. Similar tests [5] were previously performed on the old thin wall test section. The test results shown here are consistent with those previous test results.

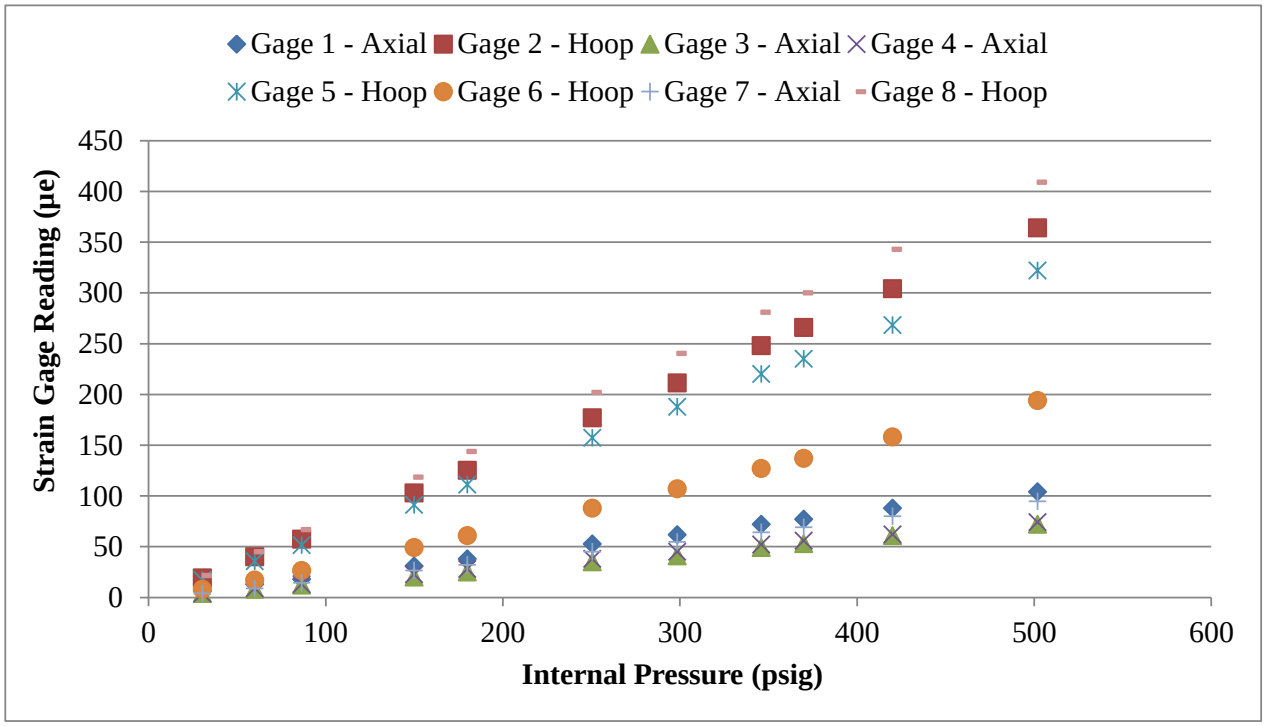

Figure 30. Strain gage pressure response test results

4.3 Strain Gage Temperature Response Test

In addition to the strain gage balance test discussed earlier, the vendor also performed temperature response tests for the strain gages. Similar tests were performed on site. Figure 31 shows the setup of the tests. The test section was laid on the test bench with two ends free to expand. Ceramic band heaters were used for the heating with the two ends covered with ceramic fiber blankets. Adjustable supports were used at the two ends of the test section to ensure that the test section was concentric with the band heaters. The test results are shown in Figure 32 to Figure 34, along with the test data from the vendor. As can be seen, the agreement is good at low temperatures. At elevated temperatures, especially at ~ 300°C, there are some discrepancies between the test data and vendor data. The vendor used a furnace for their tests, while ceramic band heaters were used for the on-site tests. Those discrepancies were probably due to the non-uniform heating in the on-site tests. Nevertheless, the overall agreement is good and acceptable.

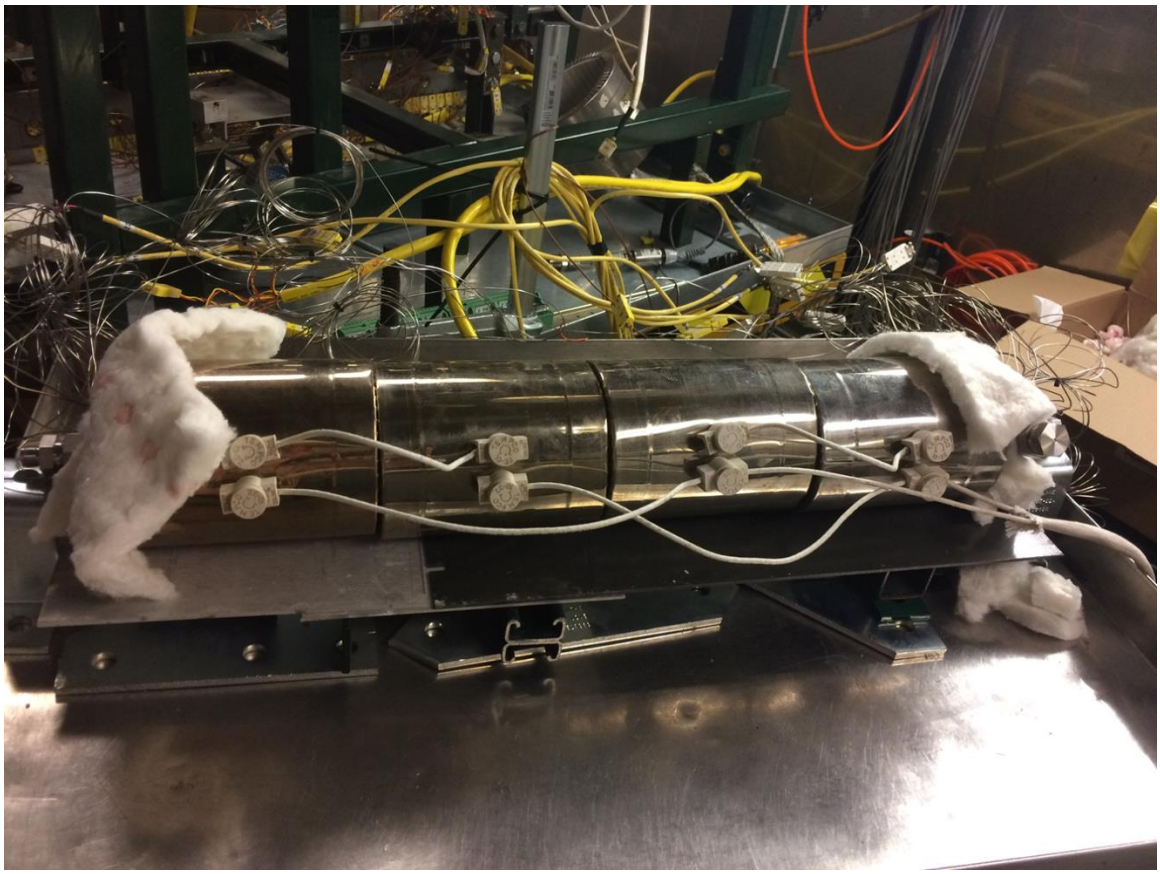

Figure 31. Setup of the strain gage temperature response test

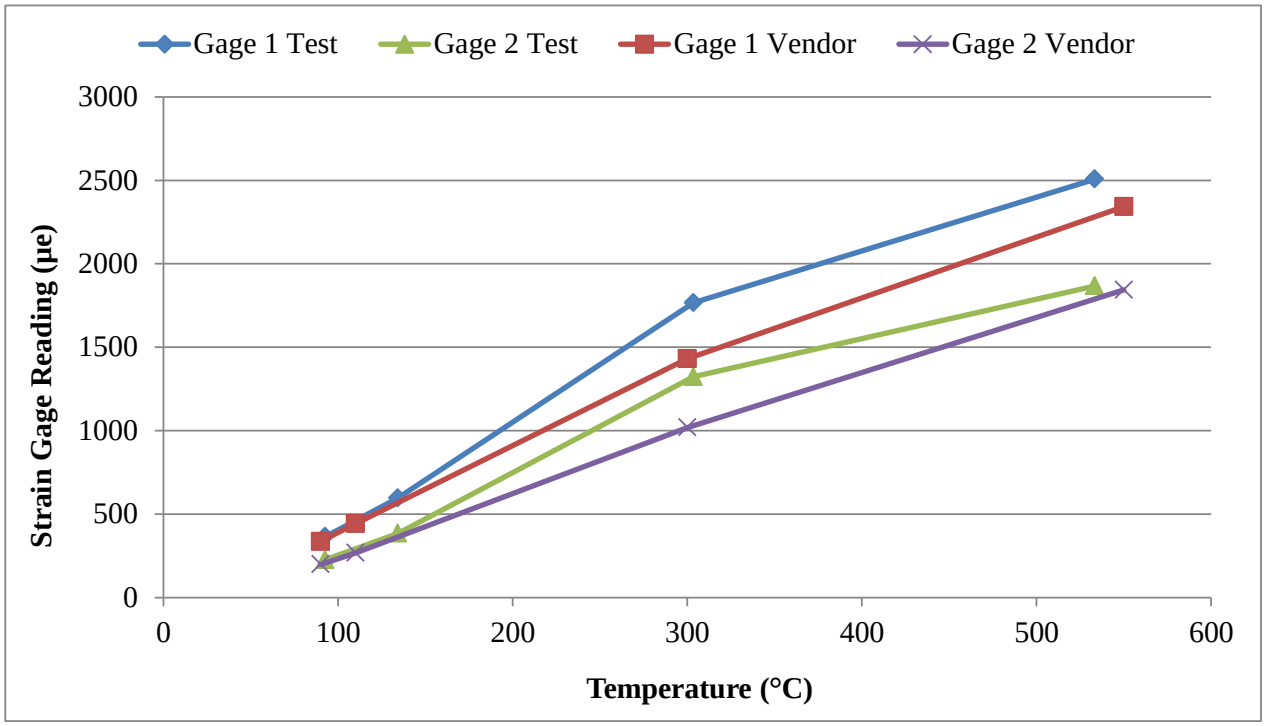

Figure 32. Temperature response test results for the two strain gages at + 4.8”

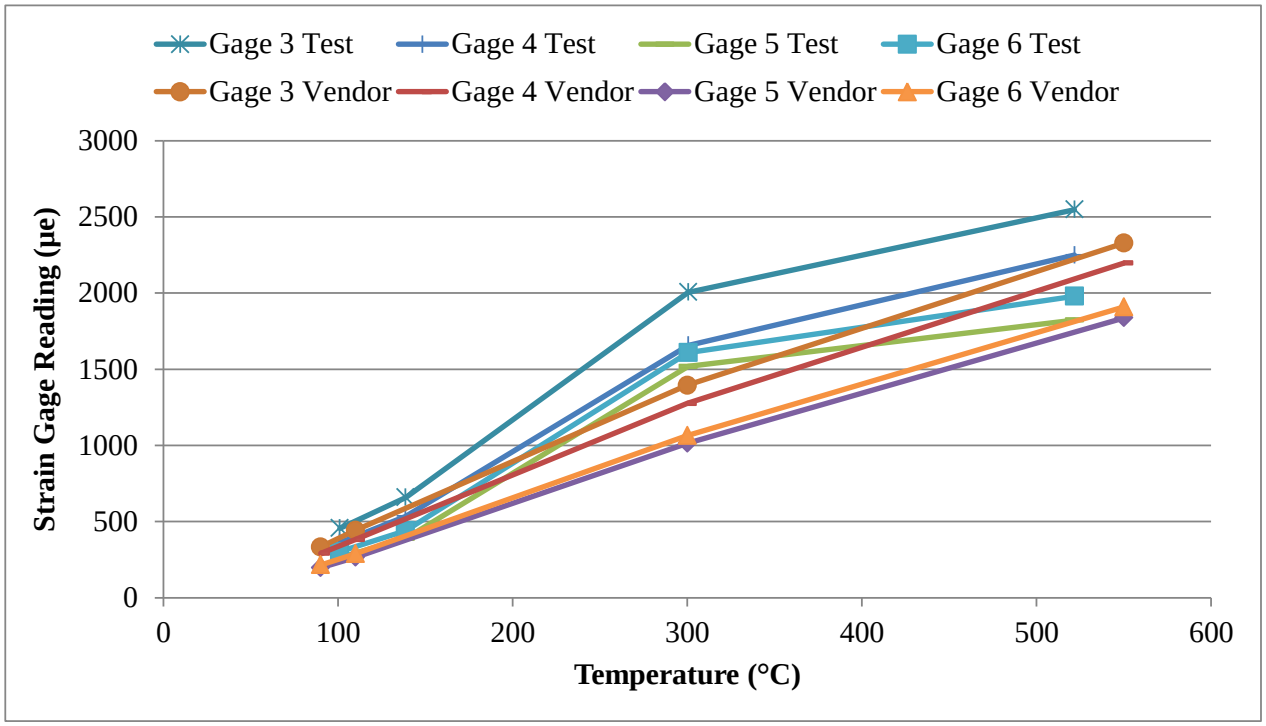

Figure 33. Temperature response test results for the two strain gages at the center

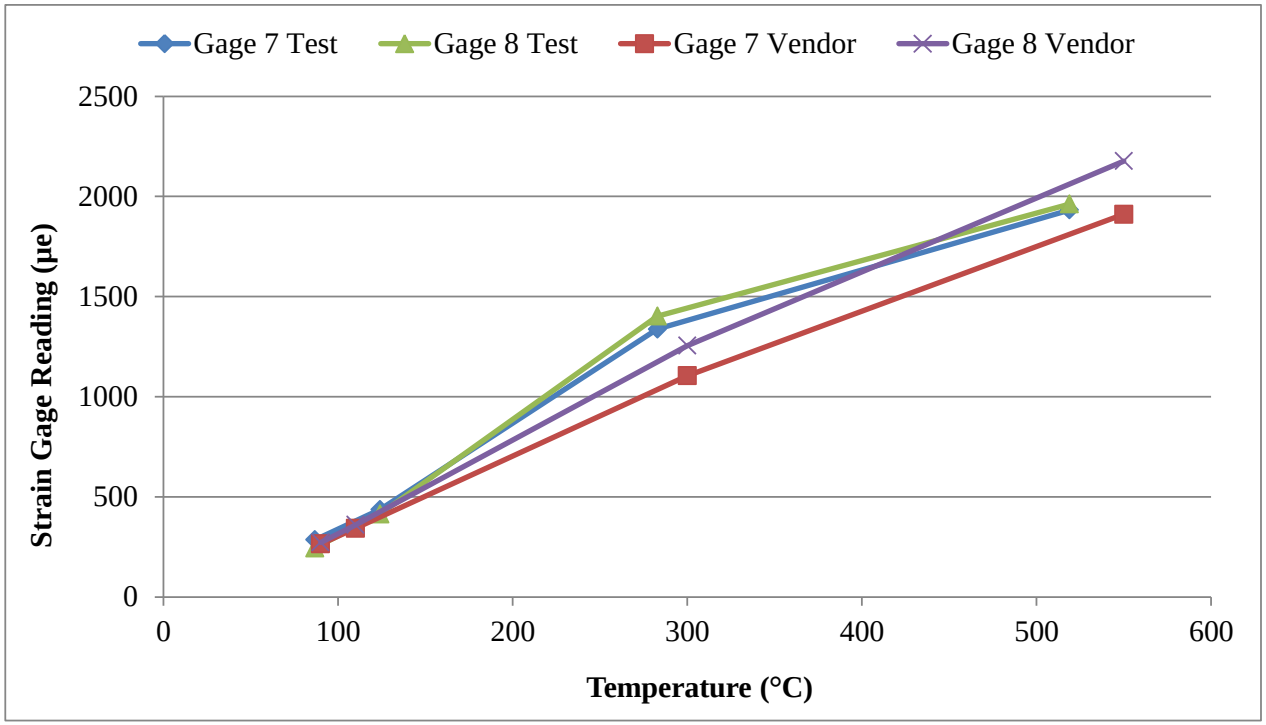

Figure 34. Temperature response test results for the two strain gages at - 4.8”

5 Shakedown Test

During the disassembly of the old test facility, glove bags were used when breaking a VCR connection to avoid causing significant contamination (oxidation) of the sodium inside the loop. Even though all the disassembly and reassembly work has been performed quickly and carefully, contamination is inevitable. The contamination can potentially cause plugging of the loop. Therefore, upon completion of the reassembly of the new test facility, it was decided to first perform a shakedown test, mainly to confirm and establish the sodium flow. In the present Sodium Freezing and Remelting test facility, there is no flow meter implemented. The only indirect way that has been employed to confirm sodium flow is intentionally heating the different zones (see Figure 20) to different temperatures. By turning on the EM pump, if a sodium flow exists, the different zone temperatures should converge to approximately the same temperature. In this shakedown test, Zone 10 was heated to ~ 250°C considering the heat sink of the EM pump magnets; Zone 12 was heated to ~ 125°C; and the rest of the loop was heated to ~ 200°C. Once the system temperatures stabilized (there were still some oscillations in the Zone 10 temperatures mainly due to the heat loss to the EM pump magnets and on-off controlling of the heaters), the EM pump was turned on. The system temperatures before and after turning on the EM pump are shown in Figure 35. As can be clearly seen, before turning on the EM pump, a temperature gradient exists along the loop. However, once turning on the EM pump, the system temperatures converge to approximately the same temperature of ~ 200°C. This clearly demonstrates that a sodium flow has been established and the loop is operational.

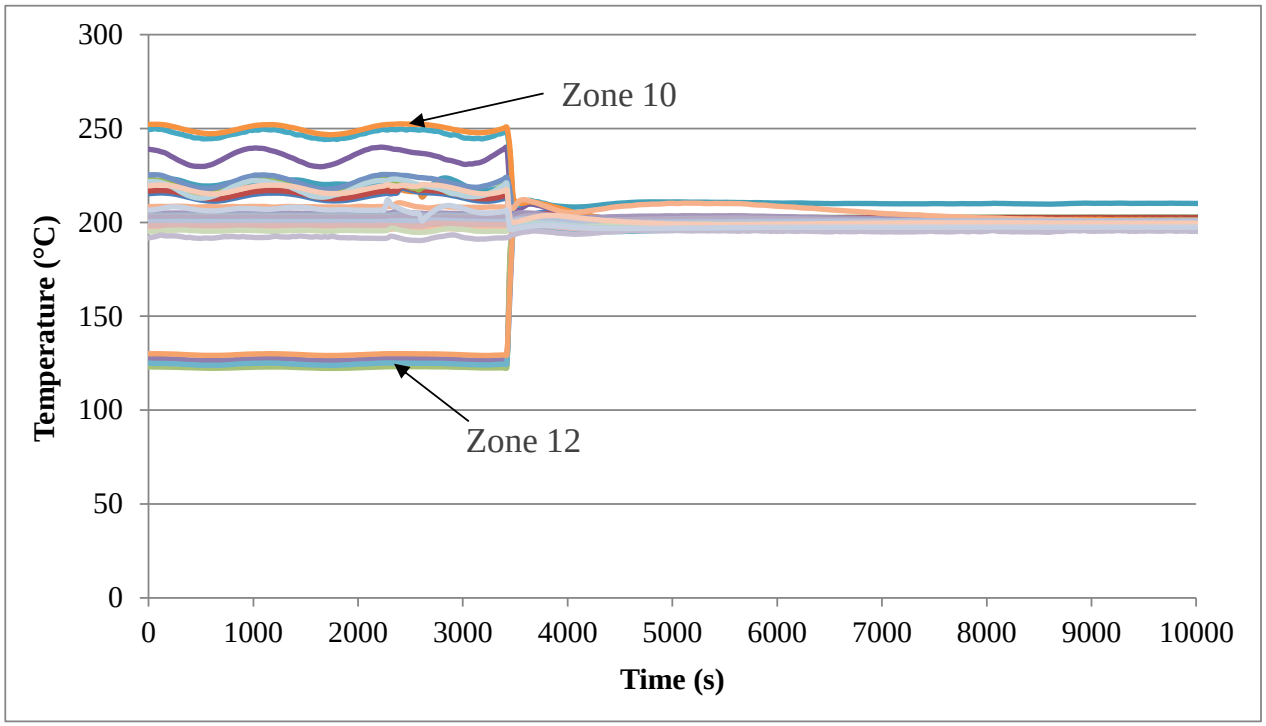

Figure 35. System temperatures before and after turning on the EM pump

6 First Freezing Test at ~ 400°C

After confirming the sodium flow in the shakedown test, it was decided to proceed with the formal tests. The Sodium Freezing and Remelting test facility has never been operated at temperatures higher than 300°C before, and therefore there was no well-established test procedure for tests at temperatures above 300°C. So the first test, although called a 'formal' test, was still a trial test, in which the test section temperatures were raised up slowly in multiple steps.

For this test, the loop was first evacuated to remove the cover gas at room temperature. This evacuation helped eliminate potential gas pocket formation in the test section as well as to reduce any dissolved gas in the sodium. It is known that the dissolved gas may become a seed of cavitation during the freezing. If such cavitation occurs, the expected inward pressure may be significantly reduced. The loop was then heated to melt the sodium from the free surfaces toward the center of the test section. Once the sodium was melted, the Zone 12 temperatures were raised to 125°C, Zone 10 temperatures to 225°C and the rest of the loop to 200°C. The EM pump was subsequently turned on, and the sodium flow was confirmed by observing the convergence of the loop temperatures. These steps were deemed as necessary to confirm sodium flow, and thus would be repeated for every future test. Once the sodium flow started, the cold finger was turned on by introducing cold air into it. The Zone 11 controller was then set to and fixed at a 150°C set temperature to keep it as the coldest region in the loop. This would ensure that the impurities deposit onto the cold finger in Zone 11, not any other region in the loop. The loop temperatures were then increased slowly in steps. With the cold finger on, there was competition between cooling and heating. Every time when the loop set temperatures (except for Zone 11) were increased, it took time for the system to stabilize and develop some temperature gradient. As the test continued and when the test section temperatures were raised to ~ 400°C, difficulties were encountered in controlling the loop temperatures. Large discrepancies in PID controller and limit controller readings were observed in Zones 3, 5, and 7. After a group discussion, it was concluded that the controlling thermocouples and heaters for those zones were not thermally coupled well, and improvement work would be needed to reposition those controlling thermocouples and heaters. It was then decided to stop increasing the system temperatures. The system was maintained at that state (~ 400°C in the test section) for approximately 2 hours (see Figure 36), before the sodium leak early warning system was triggered. When the warning system was triggered, immediate actions were taken to trace and identify the location of the VCR fitting indicating sodium leakage. The information from the warning system led to a VCR fitting in Zone 12. However, no smoke was observed at that location. Also, the heater controller set temperature was lowered for that specific zone, the temperatures there (read from both the warning system and data acquisition system) started to decrease. This did not appear to be a real sodium leak. To be cautious, it was decided to lower the system temperatures and perform a freezing test.

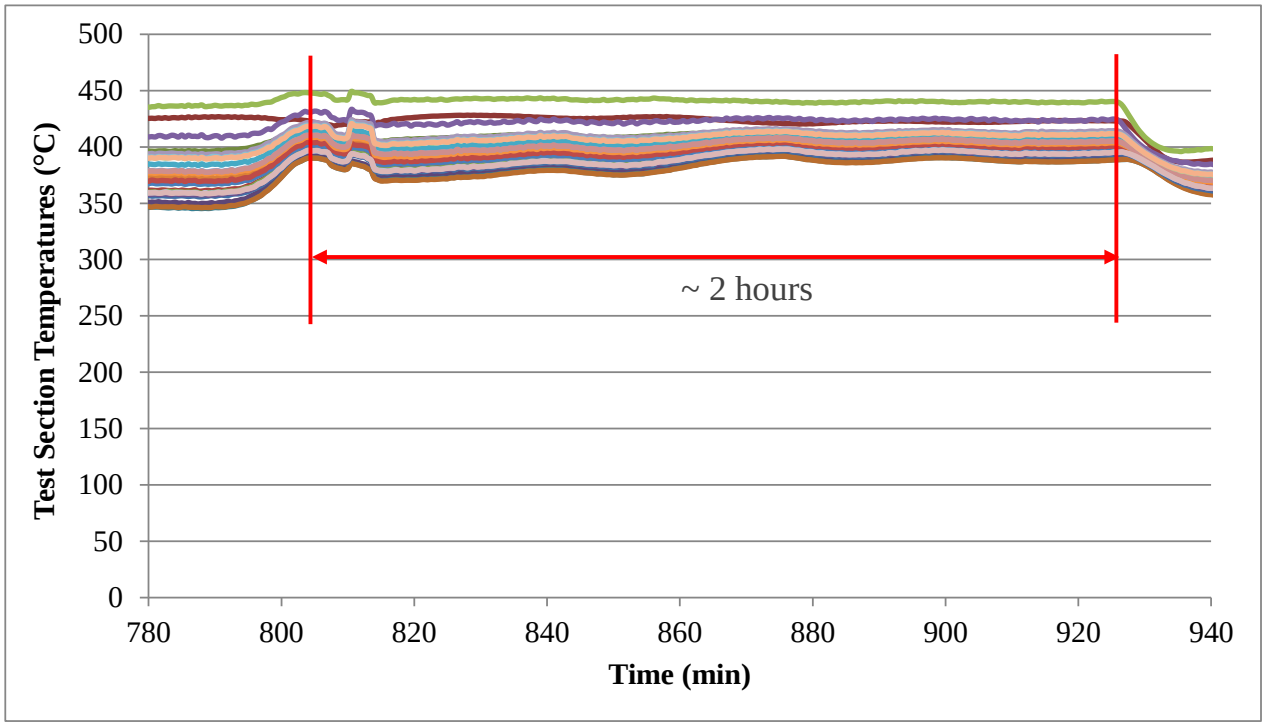

Figure 36. Test section maintained at ~ 400°C for ~ 2 hours

For the freezing test, the system temperatures were first lowered to ~ 110°C. The freezing was then started from the free surfaces by turning off the heaters in the corresponding zones (Zones 10 and 11). The free surfaces were first frozen so that the test section could detect the maximum strain change when sodium freezing occurred. When freezing started to occur in the test section, the freezing front was controlled to propagate from the ends of the test section toward its center, as shown in Figure 37.

The measured test section strains at three different axial locations during sodium freezing are plotted against the corresponding average temperature at each location, as shown in Figure 38 - Figure 45. Among the 8 strain gages, the hoop strain gage at +4.8" location (Figure 41), two axial strain gages (Figure 42 and Figure 43) at the center, and one hoop strain gage at the center (Figure 44) clearly captured the pulling effect from the freezing sodium and the subsequent breakaway of sodium from the wall. When the sodium freezes, due to its contraction, the tube first experiences a drop in the strain. However, the test section was heated to ~ 400°C for only ~ 2 hours in the present test, which was not sufficient to reach a complete wetting of the test section inner surface. Therefore, the bonding between the frozen sodium and test section inner wall was not strong enough and eventually broke, causing an increase in the tube strain. The axial strain gage at -4.8" location (Figure 38) only captured the pulling effect from the freezing sodium; the axial strain gage at +4.8" location (Figure 40), and one hoop strain gage at the center (Figure 45) only captured the breakaway of frozen sodium from the wall; while the hoop strain gage at -4.8" location (Figure 39) did not capture anything. The maximum strain change measured in the present test is ~ 10 axial micro strains, corresponding to a negative pressure of only ~ 24 psi.

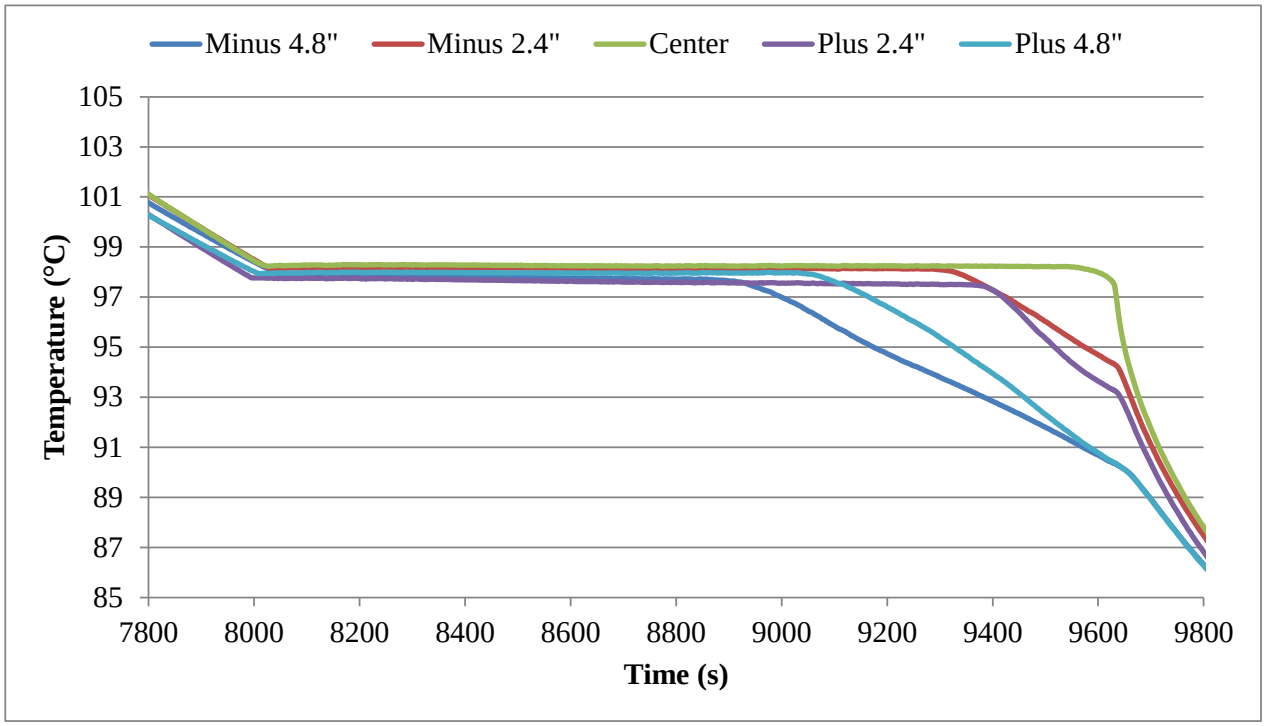

Figure 37. Propagation of freezing front from the ends toward the center of the test section

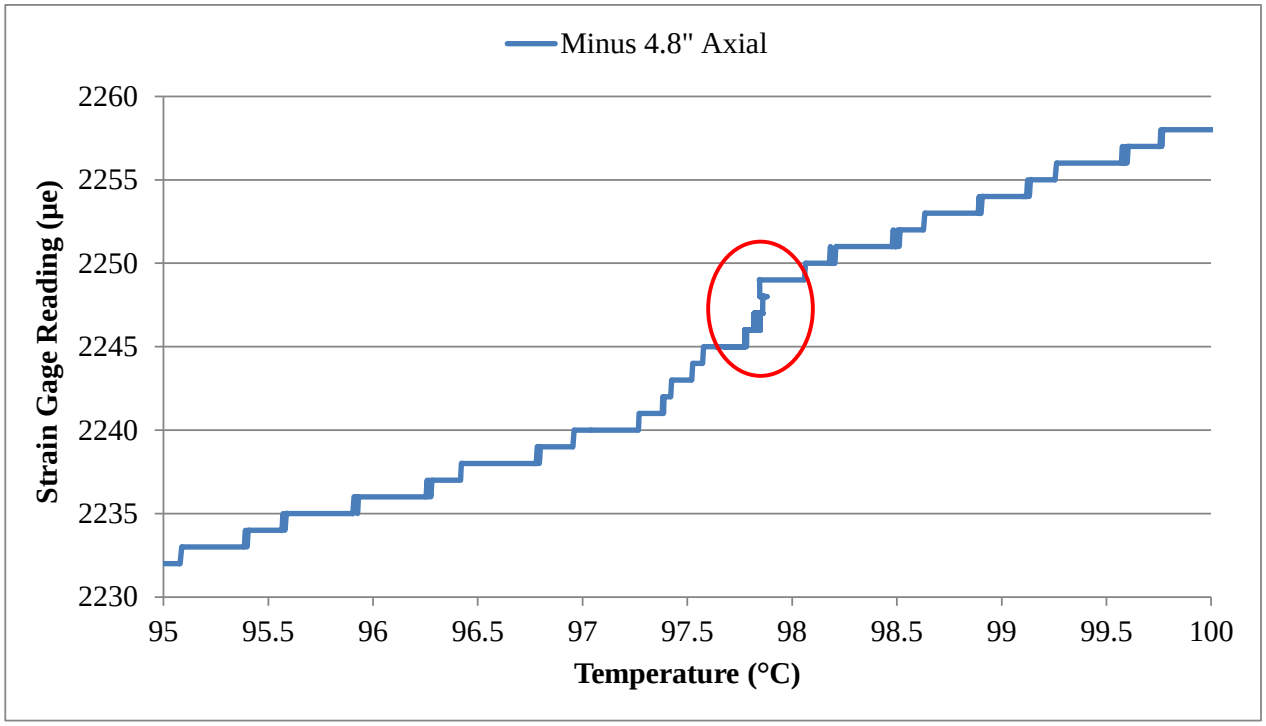

Figure 38. Axial strain vs temperature at –4.8" from the test section center

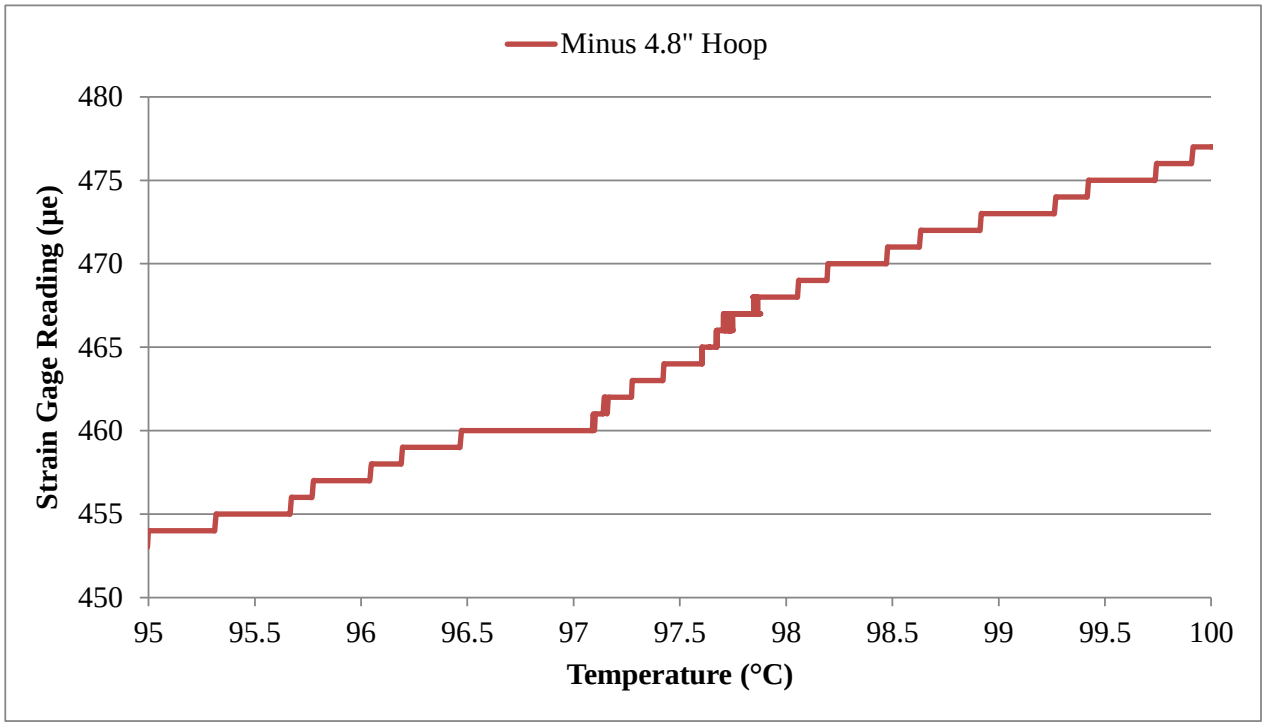

Figure 39. Hoop strain vs temperature at -4.8" from the test section center

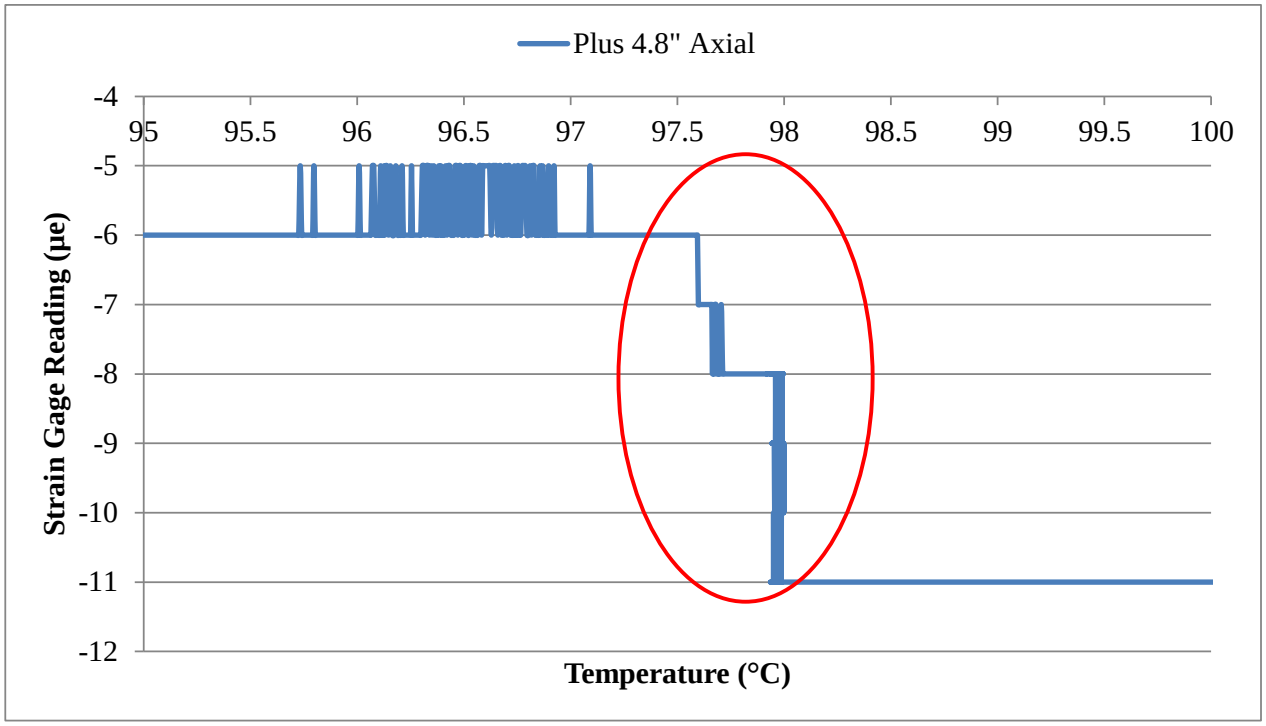

Figure 40. Axial strain vs temperature at +4.8" from the test section center

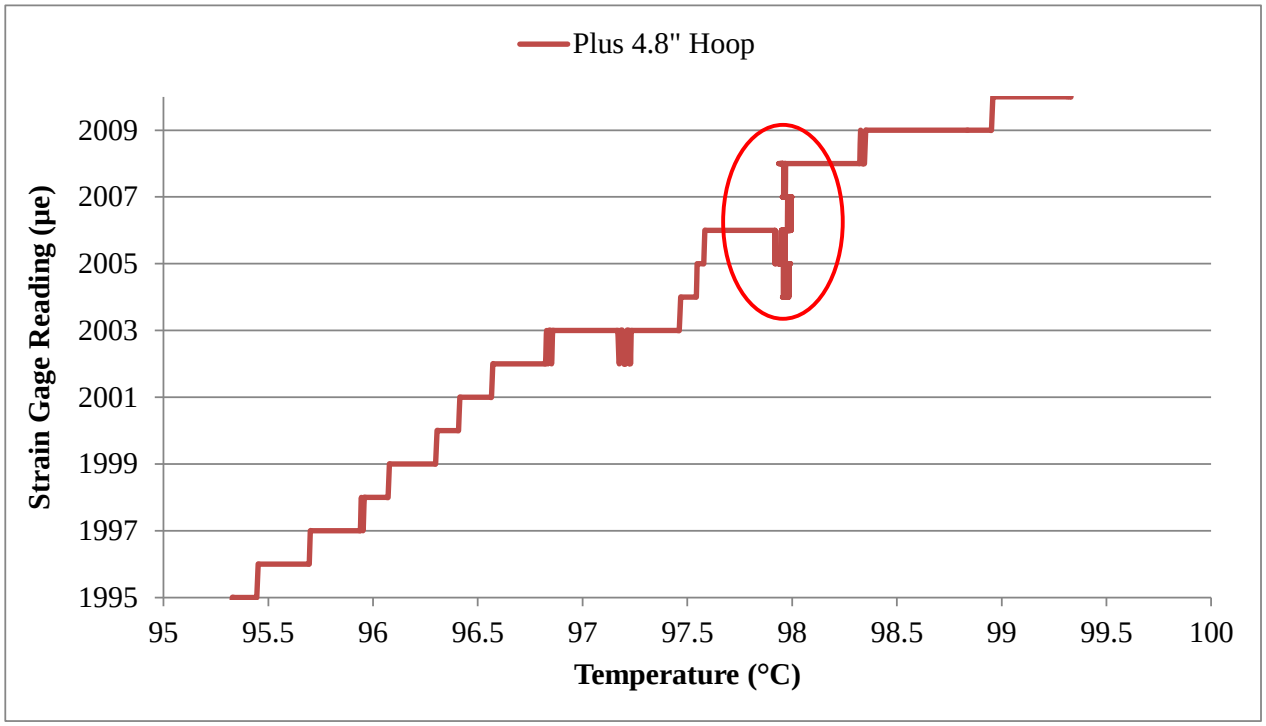

Figure 41. Hoop strain vs temperature at +4.8" from the test section center

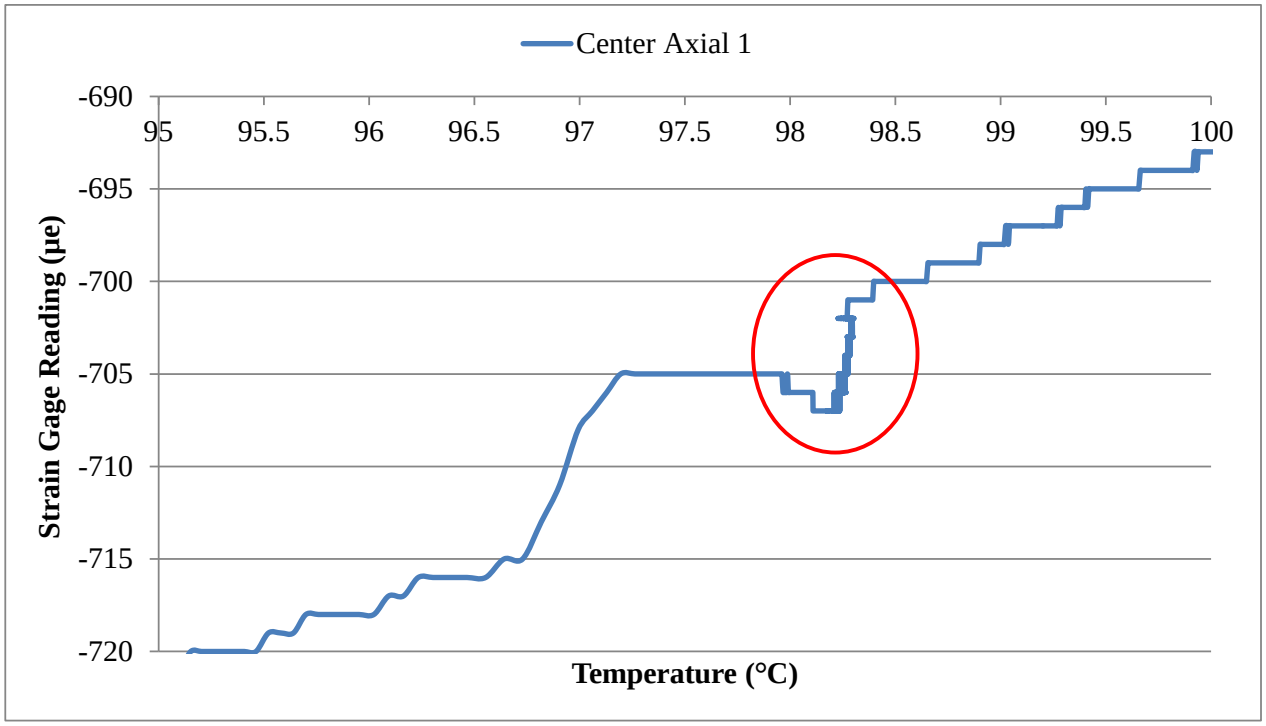

Figure 42. Axial Strain 1 vs temperature at the test section center

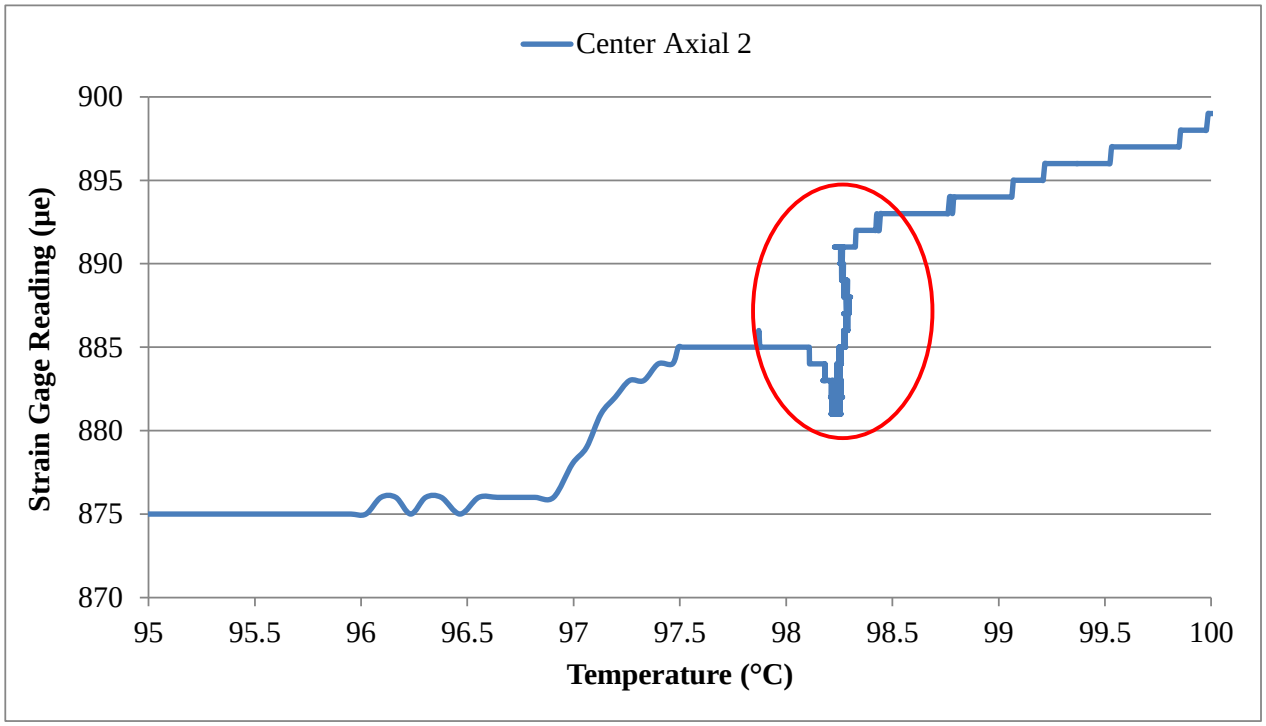

Figure 43. Axial Strain 2 vs temperature at the test section center

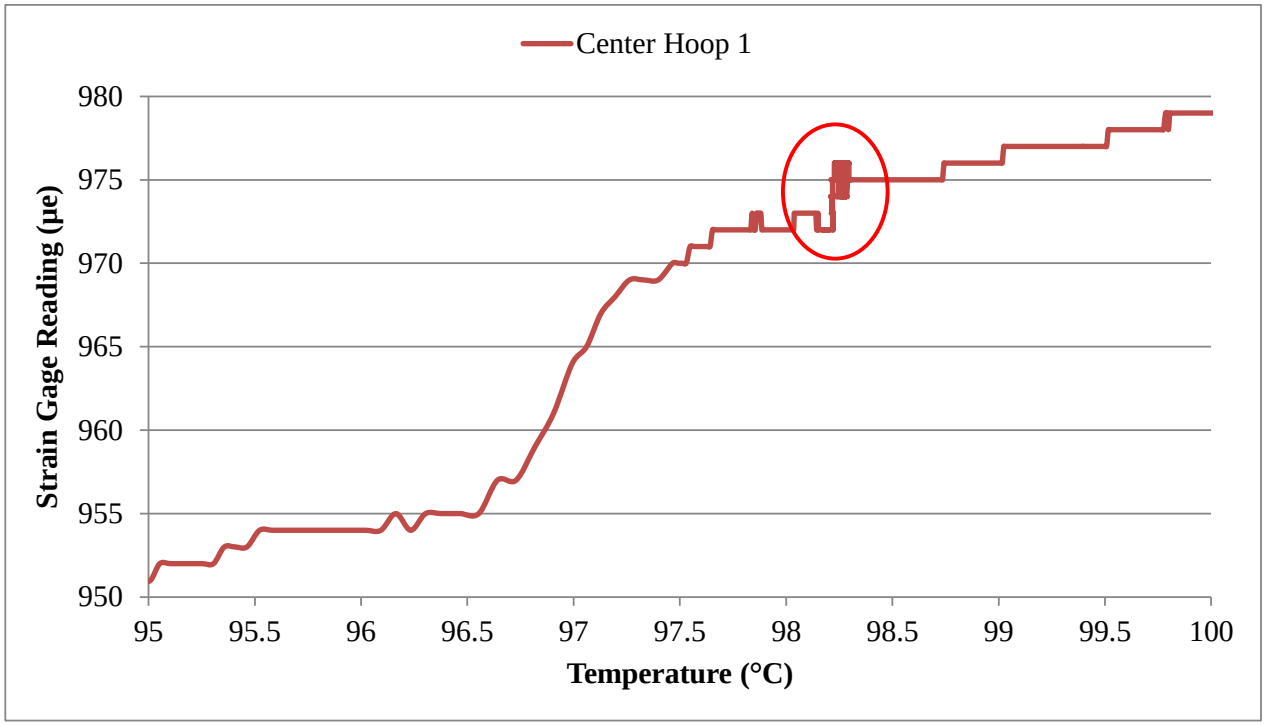

Figure 44. Hoop Strain 1 vs temperature at the test section center

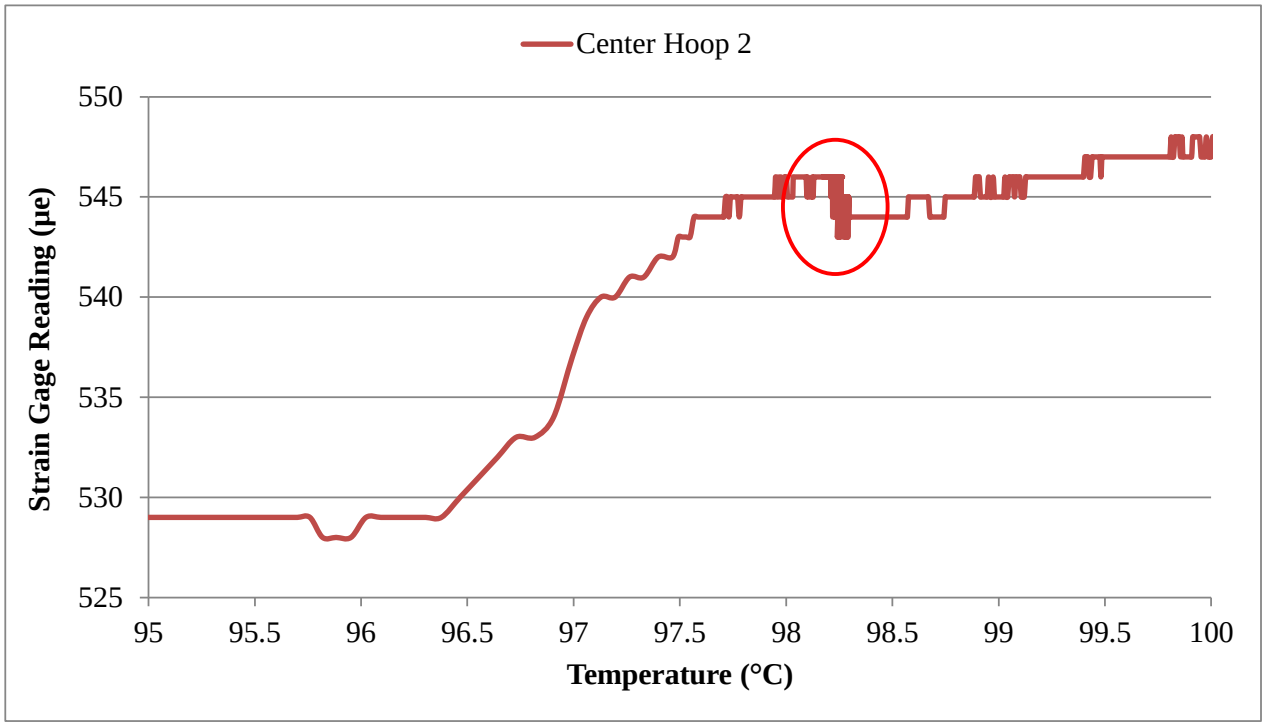

Figure 45. Hoop Strain 2 vs temperature at the test section center

7 Summary

The Sodium Freezing and Remelting experiment facility at Argonne National Laboratory has been significantly modified and improved. The main improvement was replacement of the two original stainless steel test sections that had strain gages limited by their bonds to the stainless steel to maximum temperatures of 350°C with a single new test section with strain gages that can be utilized up to 980°C and a thin wall to enhance measured strains. Wetting of stainless steel by sodium within a practical time of one to a few days is expected to require temperatures of 450°C or greater. Thus, the higher temperature strain gages enable wetting in a short time of a few days. Wetting below 350°C would have required an impractically long time of at least weeks. Other improvements included upgrading of the loop configuration, incorporation of a cold finger to purify sodium, a new data acquisition system, and reinstallation of the many heaters, heater controllers, and thermocouples. A series of baseline tests on the new test section, including the pressure response tests, temperature response tests, and strain gage balance tests were performed before and after the new test section installation. These tests provide useful baseline data for correction and troubleshooting that may be needed for subsequent formal tests. After the loop had been heated to 400°C for about two hours, an initial sodium freezing test was conducted. It is thought that the sodium might have at least partially wetted the stainless steel wall under these conditions. The strain gage measurements indicate that an incremental step inward deformation of the test section thin wall occurred as the temperature decreased through the sodium freezing temperature. This behavior is consistent with sodium initially adhering to the stainless steel inner wall but breaking away from the wall as the freezing sodium contracted. Conduct of additional sodium freezing tests under well wetted conditions was prevented as a result of stoppage of all electrical work at Argonne by the Laboratory Director on July 25, 2017. A pathway to resuming electrical work is now in place at Argonne and additional sodium freezing testing will resume next fiscal year.

Acknowledgements

Argonne National Laboratory's work was supported by the U. S. Department of Energy Advanced Reactor Technologies (ART) Program under Prime Contract No. DE-AC02-06CH11357 between the U.S. Department of Energy and UChicago Argonne, LLC. The work presented here was carried out under the Energy Conversion Technology area of the ATR Program. The authors are grateful to Gary Rochau (SNL), the Technical Area Lead, Bob Hill (ANL/NE), the National Technical Director, as well as Brian Robinson (U.S. DOE), Headquarters Program Manager for the project.

Vince Novick, Rich McDaniel, Jim Grudzinski (ANL/NE) as well as Matthew Weathered (University of Wisconsin Madison) also worked on the assembly and operation of the original Sodium Freezing and Remelting facility. The authors are indebted to them for their contributions through the preceding years.

References

[1] D. Southall and S.J. Dewson, "Innovative Compact Heat Exchangers," in *Proceedings of ICAPP'10*, San Diego, CA, June 13-17, 2010.

[2] Website of Heatric Division of Meggitt (UK) Ltd. [Online]. www.heatric.com

[3] J.J. Sienicki and C.B. Reed, "Small-scale Experiment Concepts for the Investigation of Fundamental Phenomena in Compact Sodium Heat Exchangers," ANL-GenIV-173, Argonne National Laboratory, 2010.

[4] J.J. Sienicki, C.B. Reed, S. Majumdar, Y. Momozaki, and B. Size, Argonne National Laboratory, unpublished information, 2011.

[5] C.B. Reed, J.J. Sienicki, Y. Momozaki, J.J. Grudzinski, and D.B. Chojnowski, Argonne National Laboratory, unpublished information, 2012.

[6] C.B. Reed et al., "Initial Results from Fundamental Sodium Freezing and Melting Experiments," ANL-SMR-4, Argonne National Laboratory, 2013.

[7] C.B. Reed et al., Argonne National Laboratory, unpublished information, 2014.

[8] Hitec Products, Inc. [Online]. http://hitecprod.com/hpi_products/hoskins-hbwah-series/

[9] R.P. Taleyarkhan, F. Moraga, and C.D. West, "Experimental Determination of Cavitation Thresholds in Liquid Water and Mercury," in *Proceedings of the 2nd International Topical Meeting on Accelerator Applications (AccApp'98)*, Gatlinburg, TN, USA, Septermber, 1998.

Nuclear Engineering Division
Argonne National Laboratory
9700 South Cass Avenue, Bldg. 208
Argonne, IL 60439

www.anl.gov

Argonne National Laboratory is a U.S. Department of Energy
laboratory managed by UChicago Argonne, LLC